The Effect of Mandibular Protrusion on Pediatric Temporomandibular Joint Stresses and Association with Mandibular Growth

Brandon Nguyen, DDS

A thesis submitted in partial fulfillment for the
Degree of Master of Science in Orthodontics

Oregon Health & Science University
Portland, OR

December 2023

The Effect of Mandibular Protrusion on Pediatric Temporomandibular Joint Stresses and Association with Mandibular Growth

Brandon Nguyen, DDS

Master of Science in Orthodontics Research Advisory Committee:

Signature: _____ Date: _____

Laura Iwasaki, DDS, MSc, PhD
Professor, Division of Orthodontics
Chair, Department of Oral and Craniofacial Sciences
Oregon Health & Science University

Signature: _____ Date: _____

Jeff Nickel, DMD, MSc, PhD
Professor Provisional, Graduate Program Director, Division of Orthodontics
Department of Oral and Craniofacial Sciences
Oregon Health & Science University

Signature: _____ Date: _____

Saulo L. Sousa Melo, DDS, MS, PhD
Associate Professor, Division of Oral Diagnostic Sciences
Department of Oral and Craniofacial Sciences
Oregon Health & Science University

ACKNOWLEDGEMENTS

Thank you to my colleagues, friends, and family for your continuous support.

Thank you to my thesis committee for your guidance and mentorship.

TABLE OF CONTENTS

List of Tables

List of Figures

The Effect of Mandibular Protrusion on Pediatric Temporomandibular Joint Stresses and Association with Mandibular Growth

Brandon Nguyen, DDS[a]
Hongzeng Liu, PhD[b]
Saulo L. Sousa Melo, DDS, MS,PhD[c]
Jeff C. Nickel, DMD, MSc, PhD[d]
Laura R. Iwasaki, DDS, MSc, PhD[e]

[a]Graduate Student, Department of Oral and Craniofacial Sciences, Oregon Health & Science University, Portland, OR

[b]Department of Oral and Craniofacial Sciences, Oregon Health & Science University, Portland, OR

[c]Associate Professor, Division of Oral Diagnostic Sciences, Department of Oral and Craniofacial Sciences, Oregon Health & Science University, Portland, OR

[d] Professor Provisional, Graduate Program Director, Division of Orthodontics, Department of Oral and Craniofacial Sciences, Oregon Health & Science University, Portland, OR

[e]Professor, Division of Orthodontics, Chair, Department of Oral and Craniofacial Sciences, Oregon Health & Science University, Portland, OR

Keywords: temporomandibular joint, loading forces, joint stresses, functional appliance, mandibular growth

1) Abstract

Title: The Effect of Mandibular Protrusion on Pediatric Temporomandibular Joint Stresses and Association with Mandibular Growth

Objectives: In a pediatric population before orthodontic treatment, to determine if there were: 1. significant differences in A. predicted TMJ loads (% applied bite force (BF)) and B. estimated TMJ compressive stresses (σ, MPa) during unilateral biting on molars with the mandible in retruded position compared to on molars and incisors with the mandible protruded to class I occlusion; and 2) correlations of A. predicted TMJ loads and B. estimated TMJ compressive stresses with dependent variables of sex, age, mandibular plane angle, ramal length, and/or mandibular length.

Materials and Methods: According to OHSU Institutional Review Board oversight, subjects were enrolled based on inclusion criteria: age 10-14 years; skeletal Class II malocclusion with treatment plan for fixed orthopedic appliance therapy to promote mandibular growth; permanent teeth erupted with, at a minimum, permanent incisors and first molars present; cervical vertebral maturation stage 2-3; and exclusion critera: history of TMJ trauma, musculoskeletal disease, or craniofacial anomaly; teeth with conditions that would impair participation (caries, large restorations, marked mobility); and inability to follow written or auditory instructions. Cone-beam computed tomographic (CBCT) images were made and used to: estimate mandibular condylar rectilinear loading area based on axial plane dimensions: major axis X minor axis (mm^2); measure mandibular plane angle (Frankfort horizontal to mandibular plane); ramal length (condylion to gonion); and mandibular length (maximum length of condyle to pogonion, mm); and construct three-dimensional anatomical geometry files of the positions of mandibular condyles, teeth, and positions and orientations of masseter, temporalis, medial and lateral

pterygoid, and digastric muscles. Computer-assisted numerical models, with the objective of minimization of joint loads or muscle effort, were used with subject-specific geometry files to predict TMJ loads for a static-bite force of 10 N applied at a range of biting angles on the mandibular right first molar in the retruded and protruded mandibular positions and the central incisor in the protruded mandibular position. Estimated TMJ compressive stresses (N/mm^2, MPa) were calculated using the predicted TMJ loads divided by the estimated condylar loading area for the ipsilateral (right) and contralateral (left) mandibular condyles in each subject. Two-sample and paired t-tests were used to evaluate differences in TMJ loads and estimated compressive stresses for molar and incisor biting in the retruded and protruded mandibular positions, where $p<0.05$ was considered statistically significant. Regression analyses were used to test for correlations of TMJ loads and of compressive stresses with sex, age, mandibular plane angle, ramal length, and/or mandibular length.

Results: Seven males and five females met inclusion criteria and did not meet exclusion criteria. Intraclass coefficients determined excellent intrarater reliability. TMJ loads and compressive stresses were significantly greater for incisor biting in the protruded mandibular position compared to molar biting in the protruded mandibular position (all $p\leq0.002$ and $p<0.001$, respectively). For pooled biting conditions and sexes, within condyle sides, there were no significant differences in TMJ compressive stresses between unilateral molar biting in the retruded and protruded mandibular positions (all $p\geq0.18$). There were no sex differences for TMJ compressive stresses for any of the biting or mandibular positions. Regression analyses of TMJ load (% of applied bite force) versus mandible length (mm), and Co-Go length (mm) showed positive correlations for both ipsilateral and contralateral TMJs for molar biting in the retruded mandibular position ($R^2 = 0.69$, $R^2 = 0.46$, respectively) and incisor biting in the protruded

mandibular position ($R^2 = 0.24$, $R^2 = 0.30$, respectively). Regression analysis showed increased age and decreased ipsilateral TMJ compressive stress were non-linearly correlated with increased mandibular length ($R^2 = 0.52$).

Conclusions: In a pediatric population before orthodontic treatment: 1A. Predicted TMJ loads (% applied bite force) and 1B. TMJ compressive stresses (MPa) were significantly greater during unilateral incisor biting with the mandible protruded to class I occlusion compared to unilateral molar biting with the mandible in the retruded and protruded positions, but not different during unilateral molar biting with the mandible in protruded compared to retruded position; 2A. Both ipsilateral and contralateral TMJ loads for unilateral biting on molars with the mandible in retruded position and incisors with the mandible in protruded position were positively correlated with mandibular and ramal lengths; and 2B. Increased age and decreased ipsilateral TMJ compressive stress were non-linearly correlated with increased mandibular length. Thus, increased age in the range between 10-14 years and relatively lower ipsilateral TMJ compressive stresses may be possible pre-treatment clinical indicators of predicting success with mandibular orthopedic appliances.

2) Introduction

2.1 Facial Type

Facial type assessment has been routinely used in orthodontics to predict future growth patterns and evaluate skeletal-dental relationships. The terms brachyfacial, dolichofacial, and mesofacial were introduced in orthodontic literature over 60 years ago by Ricketts.[1] The skeletal-dental relationships of brachyfacial phenotypes (short-wide, hypodivergent) are characterized by relatively short anterior and long posterior lower facial lengths, low mandibular plane angles (Frankfort horizontal-mandibular plane angle (FMA) <22 degrees), and deep anterior over-bites; whereas, those of dolichofacial phenotypes (long-narrow, hyperdivergent) are characterized by relatively long anterior and short posterior lower facial lengths, high mandibular plane angles (FMA >30 degrees), and anterior open-bites (Figure 1). Mesofacial phenotypes are characterized by average mandibular plane angles (FMA 26 +/- 4 degrees) and therefore considered to have more balanced facial profiles.

Brachyfacial and dolichofacial phenotypes exhibit developmental differences. Less condylar growth is expected in dolichofacial phenotypes and growth of the mandible is typically expressed more vertically than in brachyfacial phenotypes.[2] This results in the relatively long lower anterior compared to posterior facial length demonstrated by dolichofacial phenotypes. By comparison, more condylar growth in brachyfacial phenotypes results in increased ramus lengths and posterior facial length and anterior-superior rotation of the mandibular plane, resulting in lower FMAs compared to dolichofacial counterparts. It is postulated that the amount of growth of the condyle may therefore play a significant role in the direction of mandibular growth.

Functional differences are present in the two facial phenotypes as well. One retrospective longitudinal study used three-dimensional geometry files (Figure 2) derived from lateral and posteroanterior cephalographs of ten brachyfacial and ten dolichofacial cases made at three timepoints (average ages of 6, 12, and 18 years) for the numerical modeling of temporomandibular joint (TMJ) loads.[3] It was found that TMJ loads for a range of biting angles at 6 years of age were not different between dolichofacial and brachyfacial phenotypes. However, at older ages (12 and 18 years), dolichofacial phenotypes had significantly higher TMJ loads by ≥20% for specific biting angles and these higher TMJ loads correlated to shorter ramus lengths compared to brachyfacial phenotypes.[3] Therefore, it is postulated that differences in TMJ loads for the same biting conditions may stimulate differences in growth of the TMJ secondary cartilages and result in differences in pediatric condylar growth.

Figure 1. Dolichofacial and brachyfacial phenotypes. Distinguishing features include shorter posterior lower face (ramal) length (arrows, dashed line) compared to anterior lower face length (arrows, solid line) and steep mandibular to Frankfort horizontal (MPA) in the dolichofacial type and longer ramal length compared to anterior lower face length and flat MPA in the brachyfacial type.

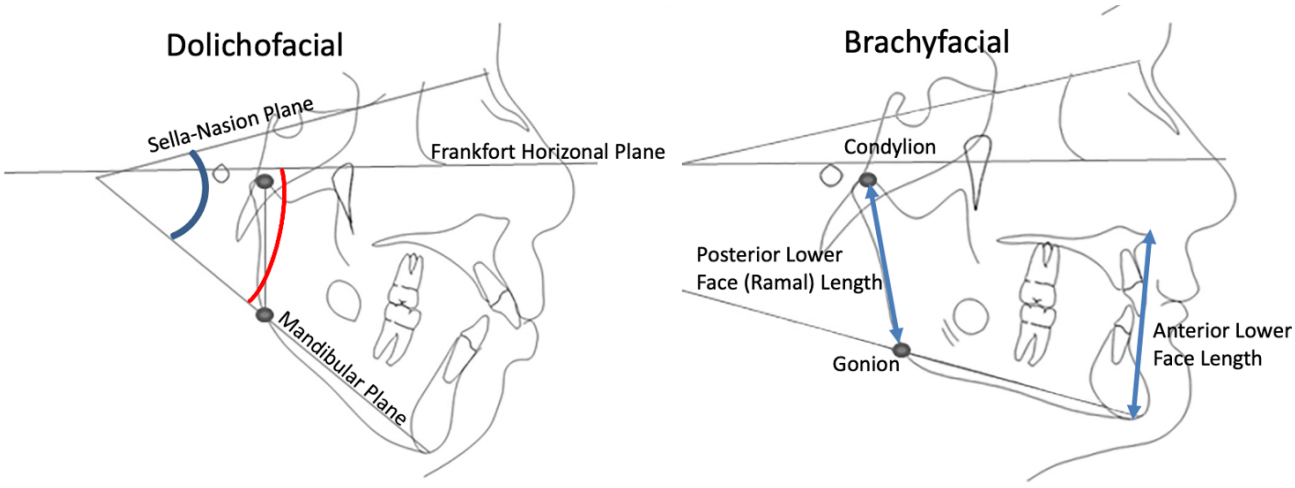

Figure 2. Three-dimensional anatomy for numerical modeling included tooth positions and force vectors for: TMJs ($F_{condyle}$; R = right, L = left), five muscle pairs ($m_{1,2}$ = masseter, $m_{3,4}$ = anterior temporalis, $m_{5,6}$ = lateral pterygoid, $m_{7,8}$ = medial pterygoid, $m_{9,10}$ = anterior digastric), and biting characterized by occlusal plane ($\theta_{xz,}$ 0–350□) and vertical (θ_y, 0– 40□) angles. Modified from [4].

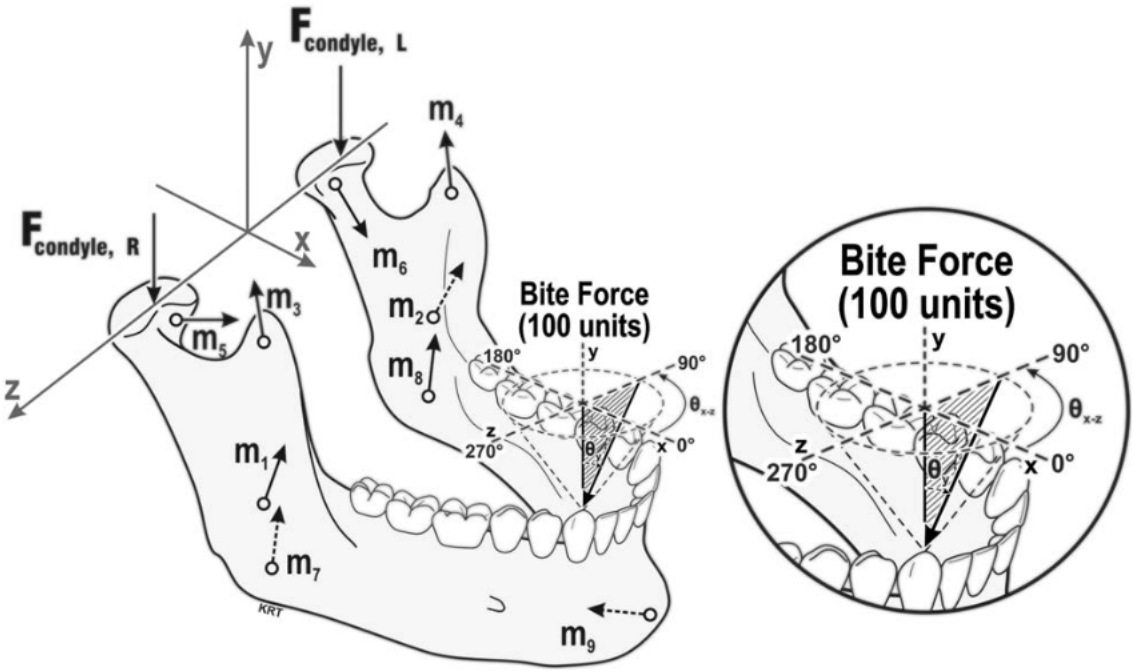

2.2 Temporomandibular Joint

Differences in TMJ loads can be a product of differences in TMJ anatomy. Compared to other post-cranial joint (hyaline) cartilage tissues, the fibrocartilages of the TMJ have higher cell densities and nutrient consumption rates and lower solute diffusivities.[5] As a result, the TMJ has steeper oxygen and glucose gradients and an increased cellular susceptibility to factors such as mechanical loading, which may impede nutrient supply and diffusivity.[6] This may suggest that external factors can affect TMJ cartilage cell proliferation. In addition, stress concentrations within the TMJ due to mechanical loading of the jaws during function are related to the congruity or surface shape-matching of the contact areas between the condyle and temporal eminence. For example, an increased congruity has been shown to be related to reduced stress

concentration associated with condyle position when biting on molars compared to biting on incisors.[7]

2.3 Functional Appliances

Orthodontic treatment of skeletal discrepancies of the retrognathic mandible may involve forward repositioning of the mandible using orthopedic appliances (functional appliances). The Herbst appliance (Figure 3) is a common functional appliance used in the correction of skeletal Class II malocclusions. Although a significant proportion of Class II correction has been shown to affect the dentition due to forward movement of the lower teeth, it has been reported that the Herbst also offers a significant skeletal effect, increasing mandibular length when compared to untreated controls.[8] It is thought that the decreased congruency (increased mismatching) of the hard tissues of the TMJ due to forward repositioning of the mandible increases the stresses and concentrations of mechanical work done (energy densities) to the loaded sites of the condyle and temporal eminence.[7] Within a range of ideal magnitudes and durations of mechanical stimulation (Figure 4), this is further thought ideally to cause cell proliferation of the mechanically-sensitive TMJ fibrocartilages at the loaded sites and endochondral bone formation leading to increased ramal length, thereby advancing the mandible forward. It has been shown that dolichofacial patients appear to respond less to Herbst appliance treatment than brachyfacial patients and remain significantly more Class II.[9] There is no literature available yet that quantifies the ideal magnitudes and durations of mechanical stimulation needed at the loaded sites to produce a therapeutic goal for a given patient. If TMJ cell proliferation is affected by external factors, it could be that stresses that are too low or too high or of insufficient or excessive duration relative

to the therapeutic threshold, and thus, may fail to promote the desired chondrogenesis and ultimately, the mandibular growth desired.

There is insufficient high-quality evidence that explains the mechanisms of dentofacial orthopedic treatment to enhance mandibular growth and the clinically notable 13-36% failure rate of this treatment, even when noncompliance is excluded.[10-13] This variance in success rates may be in part due to differences in TMJ load magnitudes and jaw-loading behaviors, affecting the frequency of loading, in different facial types. Mandibular forward positioning during skeletal Class II functional appliance treatment likely decreases TMJ hard tissue surface-mismatching.[7] This increases TMJ stress-concentrations (MPa), thereby increasing energy densities (ED, mJ/mm^3), which are measures of the mechanical work input per volume between condyle and temporal eminence loading areas. The mechanosensitivity of the growing mandibular condyle is vulnerable to the magnitude and frequency of jaw loading behaviors, measured via TMJ ED and jaw muscle duty factors (DF, muscle activity duration/total recording time, %), respectively.

Figure 3. Herbst appliance as designed in this study. Cantilever Herbst arms bilaterally extend from Rolo bands on maxillary first molars to Rolo bands on mandibular first molars, advancing the mandible forward into a more Class I occlusion. Mandibular first molar bands are soldered to a lower lingual holding arch with occlusal rests on mandibular first premolars. Maxillary first molar bands are soldered to a palatal expansion screw for maxillary expansion as indicated. If greater advancement of the mandible is desired, crimpable shims can be added to the Herbst arms. By the end of functional appliance therapy, the mandible should be advanced into a Class I or slightly Class III occlusion to account for possible relapse.

Figure 4. A theoretical model of age-dependent changes in temporomandibular joint (TMJ) compressive stresses.[6] Compressive stresses were estimated by combining age-dependent changes in TMJ loads of growing children[3] and averaged condyle size to first approximate surface areas.[14] The mechanical threshold for inhibition of chondrogenesis was estimated based on in vitro data.[15] The differences in compressive stress regression trajectories between 2 phenotypic groups suggest that the dolichofacial group reached the inhibitory threshold 3 years earlier than the brachyfacial group. This may account for phenotypic differences in jaw form and responses to mandibular orthopedic therapies.

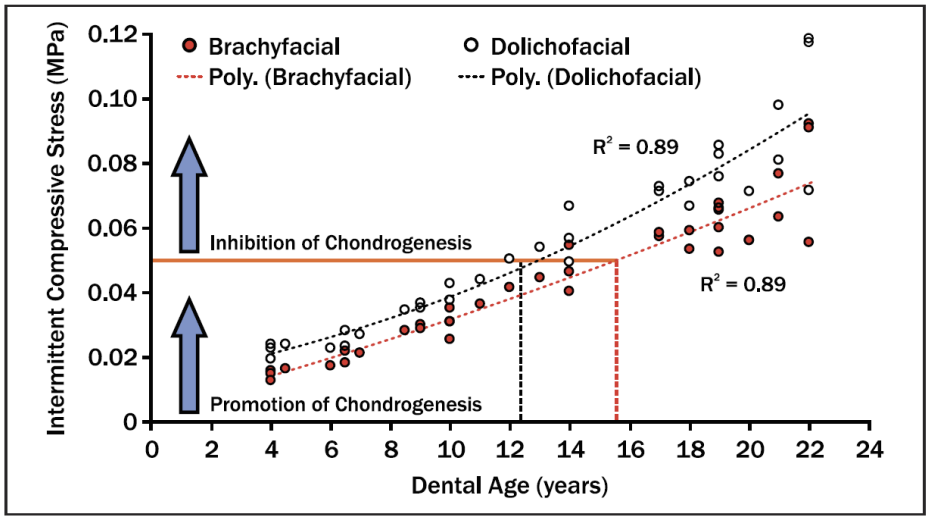

2.4 Variables of Jaw Loading

The variables of TMJ ED and DF have been combined as a mechanobehavior score (MBS=ED^{2}xDF, $(\frac{mJ}{mm^3})^2$%) and is the product of magnitude and frequency of jaw loading behaviors. It has previously been shown that MBS were correlated with ramus length in females and in males, and significantly lower and higher in two dolichofacial subgroups compared to the brachyfacial subgroup.[16]

If the MBS and component variables, such as TMJ loads and compressive stresses for the same jaw-loading task, differ between individuals, there may be inter-individual differences in the responses to similar dentofacial orthopedic treatment. Further research in the differences of energy density and frequency of loading at the TMJ contact sites between individuals undergoing Herbst treatment may elucidate the discrepancy of success rates of dentofacial orthopedic treatment. However, a first step is to consider if TMJ loads and compressive stresses are different between molar and incisor biting at the same relative applied bite forces (BFs) in retruded and protruded mandibular positions, respectively, and if these are associated with different mandibular orientations (MPA) and sizes (ramal length, mandibular length) before orthodontic treatment. Such differences could suggest potential for different amounts of mandibular growth during Herbst treatment.

2.5 Statement of the problem

To address the aforementioned gaps in evidence, this research addressed the following aims in a pediatric population before orthodontic treatment to determine if there were: 1. significant differences in A. predicted TMJ loads (% applied BF) and B. estimated TMJ compressive

stresses (σ, MPa) during unilateral biting on molars with the mandible in retruded position compared to on molars and incisors with the mandible protruded to class I occlusion; and 2. correlations of A. predicted TMJ loads (% applied BF) and B. estimated TMJ compressive stresses (σ, MPa) with dependent variables of sex, age, MPA, ramal length, and/or mandibular length.

2.6 Hypotheses

The null hypotheses tested were that there were no significant differences in 1A. predicted TMJ loads and 1B. estimated TMJ compressive stresses during unilateral biting on molars with the mandible in retruded position compared to on molars and incisors with the mandible protruded to Class I occlusion; and there were no correlations of A. predicted TMJ loads and B. estimated TMJ compressive stresses with dependent variables of sex, age, MPA, ramal length, and/or mandibular length.

3) Materials and Methods

3.1 Subjects

Subjects were patients of the Oregon Health & Science University (OHSU) School of Dentistry Orthodontic Clinic with skeletal Class II malocclusions defined by having a mandibular arch posterior relative to the maxillary arch and who were ready to begin orthodontic treatment. These patients were treatment planned for a Herbst appliance for dentofacial orthopedics (Figure 3) to promote mandibular growth.

Inclusion criteria for the study were: i) Skeletal Class II malocclusion with an orthodontic treatment plan for fixed orthopedic appliance therapy to promote mandibular growth; ii) permanent teeth erupted with, at minimum, permanent incisors and first molars present; iii) in circumpubertal stage as indicated by cervical vertebral maturation (CVM) method stage 3 (CS3) or below and between ages of 10 and 14 years at the time of initial consent. Exclusion criteria were subjects with i) a history of trauma of the TMJ; ii) a history of a musculoskeletal disease; iii) a craniofacial anomaly; iv) teeth with conditions that impaired participation in the study (dental caries, large restorations, mobility); and v) subjects who did not meet inclusion criteria.

3.2 Clinical Protocols

The clinical protocols were approved by the OHSU Institutional Review Board (STUDY00019761, Appendix A). All subjects and their legal guardians/parents provided informed assent and consent, respectively.

As a part of their orthodontic treatment planning, subjects had cone-beam computed tomography (CBCT) images made prior to beginning orthodontic treatment. During CBCT imaging, subjects wore a reference system attached to a custom bite registration appliance (monoblock; Figure 5).

Figure 5. (A) Custom occlusal registration appliance with head reference system and contrast spheres for radiographic imaging and (1) light-emitting diodes (LED). LED also attached to (2) maxillary and (3) mandibular labial tooth surfaces via custom brackets and glass ionomer cement. Modified from [17].

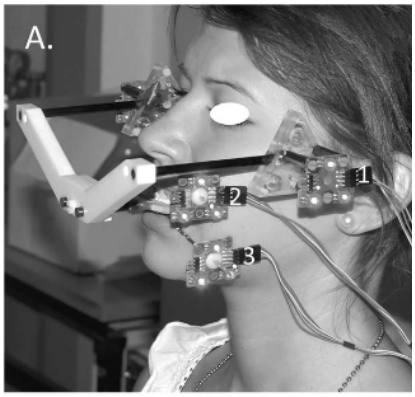

3.3 Cephalometric Measurements

Lateral cephalograms were extrapolated from pre-treatment CBCT images with available imaging software (InVivoDental, version 6.5.0). These files were then uploaded to a separate imaging software (Dolphin Imaging 11.95 Premium) to identify anatomical landmarks and quantify angular and linear measurements (Appendix B). To "close the bite" in the initial lateral cephalogram because with the monoblock in place, the subject's teeth were not in maximum intercuspation position (MIP), the "Treatment Simulation" feature of this imaging software was used to approximate the MIP depicted in the subject's initial intra-oral photographs.

The following landmarks were identified for cephalometric evaluation, using Frankfort Horitzontal plane (Porion-Orbitale) as the horizontal head reference plane (Appendix B):

- Porion (the superiormost outer bony surface point of the external auditory meatus)
- Gonion (the posteroinferiormost point on the outline of the angle of the mandible)
- Menton (the inferiormost point on the chin)
- Orbitale (the inferiormost point on the inferior margin of the bony orbit)

- Condylion (the anterosuperiormost point at the mid-mediolateral of the mandibular condyle)
- Gnathion (the anteroinferiormost point on the chin)

Mandibular plane angle (MPA,□; Figure 1) was measured as the angle from Frankfort Horitzontal plane (Porion-Orbitale) to a plane created from points Gonion to Menton to the nearest 0.1□

Ramal length (mm, Figure 6) is one measure of mandibular growth that directly reflects the growth of the condyle. Ramus length on the right and left sides in each subject was measured by two methods. Both methods used the Frankfort Horizontal plane (Porion-Orbitale) as the horizontal head reference plane. The first method quantified the linear perpendicular distance from Condylion to the occlusal plane, which was defined by the best-fit plane through the cusp tips of the mandibular posterior teeth that are fully erupted and in occlusion (Co-OP; Figure 6). The second method quantified the linear distance between Condylion on one side and Gonion on the same side (Co-Go; Figure 6). Average ramal lengths on the right and left sides were then calculated to the nearest 0.1mm.

Mandibular length (mm, Figure 6) is another measure of mandibular growth that reflects the total length of the mandible from condyle to chin. Mandibular length on the right and left sides in each subject was measured using the maximum length of the mandible from condyle to chin to the nearest 0.1 mm.

Figure 6. A. Mandibular ramal length (mm) measured on one side by two methods: a) perpendicular distance of Condylion to the occlusal plane (black lines), and b) linear distance from Condylion to Gonion (dotted line). Mandibular length (mm) is measured as the maximum length of the condyle and mandible (blue line). **B.** Example of lateral cephalography with tracing, showing occlusal plane (red line) and measurements of a) and b) (blue lines).

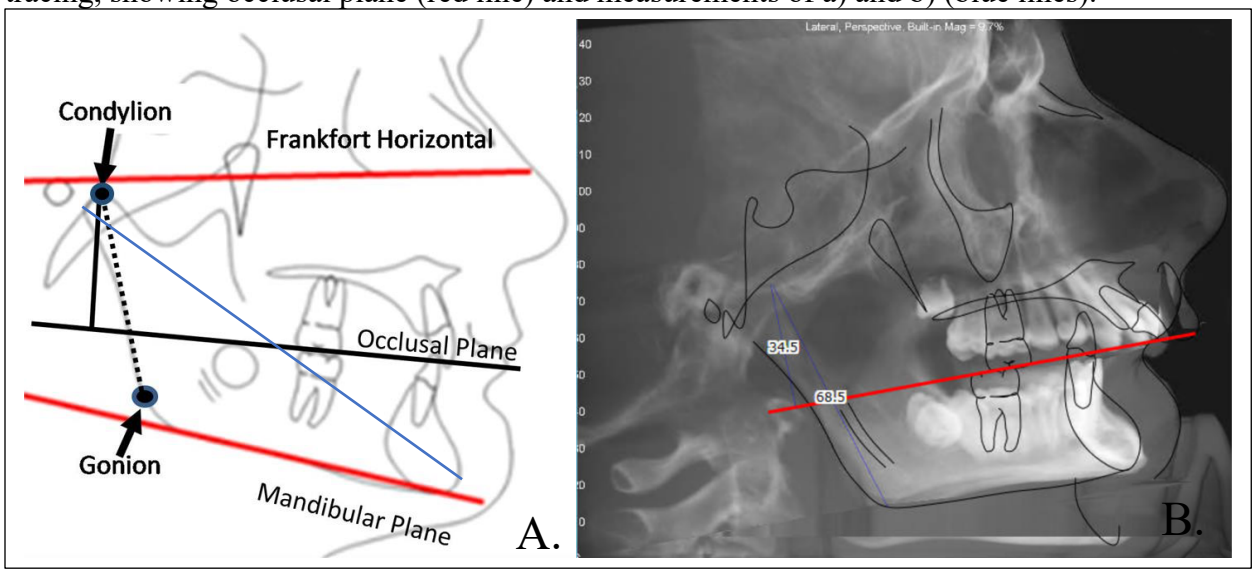

Cervical stage assessment. The cervical vertebral maturation (CVM) method was used to assess the craniofacial skeletal maturational stage of the subject. This assessment used the appearance of the second (C2), third (C3), and fourth (C4) cervical vertebrae visualized in a two-dimensional lateral cephalogram. CVM stage 3 (CS3) and CVM stage 4 (CS4) are considered to be circumpubertal[18,19]. For the purpose of this study, subjects included were CS3 and below, likely beginning treatment prior to their peak craniofacial growth velocity. This is thought to be the ideal timing for orthopedic class II correction with functional appliances.

3.4 Anatomical Geometry Files

Anatomical landmarks were identified on the CBCT images with commercially available imaging software (InVivoDental, version 6.5.0, Appendix C Figure 2). Dental, muscular, and

skeletal landmarks were included as previously described[16] and constituted a "geometry file" for use in numerical modeling to predict TMJ and muscles forces for an applied load to the mandible (Figure 2). Muscular landmarks involved attachments of muscles of mastication (masseter, medial pterygoid, lateral pterygoid, anterior temporalis, anterior digastric) to the mandible and the skull. In this approach, the term "insertion" was designated as an attachment on the mandible, and "origin" was designated as an attachment on the skull. Muscular landmarks were mainly defined as the centroid, or center of the area of attachment of the muscle at the "insertion" and "origin." Each CBCT was re-oriented according to a defined orthogonal axis system (Figure 2, Appendix C Figure 1) with reference planes created for standardization prior to landmark identification and measurement. The detailed landmark identification protocol for unilateral left-side landmarks except bilateral condyle landmarks (condylions) is described below. Unless marked asymmetry was noted, the numerical model assumed dentofacial symmetry.

<u>Identifying and labelling landmarks using software for three-dimensional (3D) analysis:</u>

1. Open CBCT file in software program.
2. To begin tracing, navigate to "3DAnalysis" tab and select "Create Tracing".
3. Landmarks are customized under "Tracing Tasks" for the purposes of this project (Appendix C Figure 2).
    1. Right condylion (supero-anterior-most point)
    2. Left condylion (supero-anterior-most point)
        i. *This is best visualized via axial clipping using "Teeth" filter to locate superior-anterior-most point.*
    3. Left mandibular central incisor (midpoint of incisal edge)

4. Left mandibular canine (cusp tip)
5. Left mandibular first molar (mid-buccal point)
6. Left masseter muscle “insertion”
    i. *Centroid of muscle attachment to the lateral surface of the inferior ramus, anterior to the angle of the mandible.*
7. Left masseter muscle “origin”
    i. *Centroid of muscle attachment to the zygomatic arch, inferior to the maxillary process of the zygomatic bone.*
8. Left medial pterygoid muscle “insertion”
    i. *Centroid of muscle attachment to medial surface of the inferior ramus, anterior to the angle of the mandible*
9. Left medial pterygoid muscle “origin”
    i. *Centroid of muscle attachment to the medial surface of the lateral pterygoid plate.*
    ii. *This is best visualized via axial clipping using the “Bone” filter*
10. Left lateral pterygoid muscle “insertion”
    i. *Centroid of muscle attachment to the medial-tending concavity of the condylar neck of the mandible.*
11. Left lateral pterygoid muscle “origin”
    i. *Centroid of muscle attachment to the anterolateral surface of the lateral pterygoid plate.*
12. Left anterior temporalis muscle “insertion”

i. *Centroid of muscle attachment to the lateral surface of the coronoid process of the mandible.*

13. Left anterior temporalis muscle “origin”

i. The field of view on most CBCT images used does not extend to temple area; therefore, landmark positioned posterior to the orbit to estimate direction of muscle pull from “insertion” to “origin”.

14. Left anterior digastric muscle “origin”

i. *Point above the superior-lateral surface of the hyoid bone lateral to the base of the lesser horn, representing the fibrous loop which the intermediate tendon passes through. The intermediate tendon links anterior and posterior digastric muscles.*

15. Left anterior digastric muscle “insertion”

i. *Centroid of muscle attachment to the left digastric fossa of the mandible*

4. Establish coordinate planes by labeling using “Coord_sys Widget” (Appendix C Figure 1).

a. Axial (x-z) plane along best fit on mandibular occlusal plane as defined by the plane intersecting incisor, canine, and molar landmarks

b. Coronal (y-z) plane intersecting right and left condylions (superoanterior points of condyles) and perpendicular to axial plane

c. Midsagittal (x-y) plane bisecting inter-condylion distance and perpendicular to axial and coronal planes

   d. Note: origin of x-y-z axis system is mid-point between right and left condylions

5. Display grid planes at 25% opacity under “Visual Preferences” tab.
6. Capture screenshots from postero-anterior (PA), axial, and left lateral views of CBCTs with landmarks and coordinate planes labelled (Appendix C Figure 3).
7. Save screenshots in designated folder and name the .jpg files according to subject identification and view: MMG###PA, MMG###Axial, and MMG###Lat, for PA, axial, and left lateral views, respectively.
8. Screenshot files ready to be accessed in a separate software program to generate geometry files.

Screenshots of the CBCT images with identified landmarks in the postero-anterior (PA), axial, and left lateral planes were then used to create 3D geometry files, which were then input to a computerized numerical model. The geometry files were created using a customized software program (MatLab, R2019a Update 4) named “GeoCreationCTM05OpenBite.m” to identify landmarks in the screenshots and quantify their position in the x-y-z axis system and to simulate maximum intercuspation jaw positions without the monoblock in place. Geometry file creation in detail is explained below.

<u>Geometry file creation using GeoCrCTM05OpenBite</u>

1. Launch custom software program: “GeoCrCTM05OpenBite” and follow instructions for identifying traced landmarks and standard measurements for calibration
   a. Horizontal and vertical ruler lengths: 5 grid units

   b. Screenshots must be named appropriately and saved in designated folders to be identified and opened by the custom software program.

2. Avoid distortion of image when enlarging CBCT screenshots
3. All “insertions” are on the mandible and represent the centroid of the main area of muscle attachment.
4. All “origins” indicate the main direction of the muscle vectors, that is, the direction of muscle pull when activated from the “insertion” to the centroid of the main area of muscle attachment on the skull or hyoid bone. This means that the actual location of the “origin” (on the skull or hyoid boid) is not as critical as choosing a point that represents the muscle vector/direction of muscle pull.
5. Because the monoblock was in place at time of CBCT capture, “condyle rest position” must be identified to estimate position of condyle without the monoblock in place. This is estimated using clinical intraoral photographs and dental models in maximum intercuspation.
6. “Supramaxillary” (maxillary) landmarks identified as points of occlusion of the mandibular incisor and molar. These are estimated using clinical intraoral photographs and dental models in maximum intercuspation.
7. Following completion of software program steps, a geometry file is generated and can be opened with text software (WordPad, version 21H2). The three columns represent x, y, z coordinates for the anatomical landmarks in which
   a. I = insertion of muscle (centroid of muscle attachment on mandible)
   b. Lambda = coordinates define the direction of the muscle vector.

3.5 Predicted TMJ Compressive Stresses

Numerical Modeling to Predict TMJ Loads

The geometry files were used by computerized numerical models to predict 1) subject-specific sagittal effective eminence shapes based on the objective of minimization of joint loads, and 2) masticatory muscle forces and TMJ forces (loads) during static biting for a range of unilateral right mandibular molar and incisor biting tasks with a bite force of 10 N applied with the mandible in the retruded and protruded positions, respectively, based on the objective of minimization of muscle effort (Figure 2).[4,20] A 10 N bite force was selected because it has been shown using electromyography recording data that during the day and night, children in their usual environments rarely showed magnitudes of tooth loading forces >8 N.[21] These objective functions have produced accurate results in validation studies.[20,22]

Each subject's geometry file was used in the numerical model as a first step, to prescribe a third order polynomial, which depicted the sagittal effective eminence shapes using published methods[23]. This model predicted TMJ load directions for bilateral vertical biting at molars to incisors in 20 sequential steps, where mandibular positions represented retrusion to protrusion. For equilibrium at each position, the eminence surface must be perpendicular to the force; therefore, the series of 20 lines perpendicular to the predicted TMJ loads were delineated and fit to a polynomial.

Each subject-specific eminence shape and geometry file was then used in a numerical model as a second step, to calculate masticatory muscle and TMJ forces for static biting on right (ipsilateral) first molars with the mandible in the retruded (MIP, Class II) and protruded (to Class I)

positions, and central incisors with the mandible in the protruded (to Class I) position. The amount of protrusion was dependent on the amount of advancement needed to achieve a class I molar (half-cusp Class II advanced 3 mm, full-cusp Class II advanced 6 mm). Bite forces were applied over a large range of angles, accounting for those likely to occur during normal jaw activities: 0–350□in the occlusal plane (θ_{xz}) in 10□steps, and angles relative to vertical (where θ_y = 0□) of 0–40□in 5□steps (Figure 2). Predicted ipsilateral (right) and contralateral (left) TMJ loads were calculated for the full range of biting angles at each biting position (molar, incisor) and mandibular position (retruded, protruded) for each subject.

Predicted TMJ loads (% applied bite force (BF)) were then used for calculations of ipsilateral and contralateral TMJ compressive stresses (σ, MPa) for subjects before orthopedic appliance therapy with the mandible in two positions: retruded (0 mm) and protruded (+Δ_x mm) to Class I dental relations, using the following equation:

$$\delta = \frac{TMJ\ load\ (\%\ BF)}{Condylar\ loading\ area\ (mm^2)}.$$

Condylar Loading Area

Condylar loading areas (mm^2) for right and left TMJs were calculated as the product of the major condylar axis (longest medial-lateral pole distance in a plane parallel to the occlusal plane) and minor condylar axis (shortest distance perpendicular to major TMJ axis). The condylar axes of both condyles were identified and measured on the CBCTs for all subjects to the closest 0.1 mm. A three-dimensional rendering of the condyle using imaging software (InVivoDental, version 6.5.0) was used to identify the longest medial-lateral distance of the condyle (major TMJ axis)

parallel to the occlusal plane. The minor TMJ axis was then measured perpendicular to the major TMJ axis within that same plane.

4) Data and Statistical Analyses

Variables considered for each subject were: sex, age, CVM, MPA (°); and for right and left sides: ramal length (Co-OP, Co-Go; mm), mandibular length (mm), condylar major axis (mm), condylar minor axis (mm), and condylar loading area (mm^2). Descriptive statistics including means and standard deviations were calculated for predicted TMJ loads (% applied BF) and TMJ compressive stresses (σ, MPa) of both right and left TMJs for a range of biting angles on right molars in a retruded jaw position and right molars and right central incisors in protruded jaw positions of 3 mm or 6 mm, dependent on the amount of advancement needed to achieve a class I occlusion. This was compared with subjects' sex, cervical vertebral maturation, age, mandibular position (retruded and protruded), ramal length and mandibular lengths for correlation. Mandibular position was analyzed separately (retruded, 3 mm protruded, 6 mm protruded) and in groups (Group A = retruded, Group B = protruded 3 mm and 6 mm).

Two-sample and paired t-tests were used to evaluate differences in predicted TMJ loads and compressive stresses during molar and incisor biting in the retruded and protruded mandibular positions, respectively. Univariate analysis of variance (ANOVA) with honest significant difference post-hoc tests (HSD) were used to evaluate between subject-effects of MPA, ramal length, mandibular length, condylar loading area, and side on predicted TMJ loads. $p<0.05$ defined significance for all statistical tests.

3D regressions were made to identify correlations between ipsilateral and contralateral TMJ loads (% applied BF) and compressive stresses (MPa) during molar biting and incisor biting with sex, age, MPA, ramal length, and mandibular length at T1.

Intraclass correlation coefficients (ICCs) were calculated to determine intrarater reliability. One judge measured MPA, ramal length (Co-Go), mandibular length, and condyle loading area twice for all subjects, with one week between measurements.

5) Results

5.1 Intra-rater reliability analysis

Tests of intra-rater reliability showed excellent reliability, where ICCs for measuring MPA, ramal length, mandibular length, and condylar loading area were all 0.99 (Table 1).

Table 1. Intrarater reliability analysis, where MPA indicates Frankfort horizontal-mandibular plane angle; Co-Go, condylion-gonion, where R indicates right (ipsilateral) and L indicates left (contralateral).

Measurement	Intraclass Correlation Coefficient (ICC)
MPA (°)	0.99
Co-Go (mm)	0.99
Mandibular length (mm)	0.99
Condyle R major axis (mm)	0.99
Condyle R minor axis (mm)	0.99
Condyle L major axis (mm)	0.99
Condyle L minor axis (mm)	0.98

5.2 Sample Description

At time of data analyses, 12 subjects (seven males, five females) in an ongoing study met the inclusion criteria and did not meet exclusion criteria and had pre-treatment CBCT images. Ages ranged from 10.3-14.9 years (average ± standard deviation (SD) of 12.8 ± 1.4 years) and CVM 2-3 (Table 2). Mandibular plane angles ranged from 9.1-23.2□(16.5 ± 5.0□), ramal length ranged from 32.2-46.4 mm (Co-OP, 38.1 ± 4.2 mm) and 51.4-70.1mm (Co-Go, 58.2 ± 5.0 mm), and mandibular length ranged from 100.1-127.6 mm (114.2 ± 6.8 mm) (Table 2). Average condylar loading area ranged from 120.7-203.4 mm^2 (166.9 ± 25.6 mm^2) (Table 3).

Table 2. Descriptive data and mandibular measurements for subjects before orthodontic treatment (T1), where CVM indicates cervical vertebral maturation stage; MPA, Frankfort horizontal-mandibular plane angle; Co-OP, condylion-occlusal plane; Co-Go, condylion-gonion; M, male; F, female; SD, standard deviation.

Subject	Sex	Age (years)	CVM	MPA (°)	Ramal Length (mm)				Mandibular Length (mm)	
					Co-OP Right	Co-OP Left	Co-Go Right	Co-Go Left	Right	Left
MMG001	M	13.3	3	13.5	37.9	40.9	55.4	54.1	117.0	116.5
MMG002	M	10.3	2	22.3	34.0	34.1	53.2	51.4	111.6	111.1
MMG003	M	14.3	3	9.4	39.8	40.2	66.3	62.8	123.0	123.1
MMG004	F	14.3	3	11.3	38.6	38.2	56.0	55.5	112.7	113.6
MMG005	F	12.4	3	17.0	32.6	33.1	55.4	57.9	109.3	109.7
MMG008	M	12.0	2	18.1	36.0	36.2	57.8	54.0	113.4	113.1
MMG009	M	14.9	3	20.0	42.6	43.5	70.1	67.4	127.4	127.6
MMG010	M	13.0	3	9.1	46.4	46.1	62.7	57.8	116.3	113.5
MMG011	F	13.3	3	23.2	33.1	32.2	55.1	52.2	100.5	100.1
MMG012	M	12.6	2	22.0	33.8	32.8	56.2	59.5	111.7	110.6
MMG013	F	11.8	2	12.6	38.1	38.1	54.5	55.1	109.0	108.3
MMG014	F	10.8	2	19.1	38.4	37.8	53.1	51.4	105.4	105.0
Average ± SD		12.8±1.4	2.6±0.5	16.5±5.0	38.0±4.1	38.3±4.4	59.5±5.9	56.8±4.8	114.4 ±6.8	114.0 ±6.9

Table 3. Condylar measurements for subjects before orthodontic treatment and overall average ± standard deviation (SD) for group.

Subject	Condylar Axis (mm)				Condylar Loading Area (mm^2)	
	Major		Minor			
	Ipsilateral	Contralateral	Ipsilateral	Contralateral	Ipsilateral	Contralateral
MMG001	21.9	22.6	8.8	7.7	191.4	172.6
MMG002	23.7	23.5	7.1	7.2	135.6	136.0
MMG003	18.9	18.9	10.6	10.1	200.3	191.0
MMG004	20.3	19.6	9.9	9.9	201.6	194.1
MMG005	19.2	19.4	8.0	6.8	154.1	131.9
MMG008	18.7	18.0	10.5	9.0	195.6	161.9
MMG009	21.6	21.5	8.3	9.5	179.7	203.4
MMG010	16.8	16.7	7.5	7.2	126.5	120.7
MMG011	18.2	19.2	8.2	8.2	149.2	157.1
MMG012	18.0	18.7	10.4	10.1	188.4	188.7
MMG013	18.4	19.2	9.0	9.5	164.2	181.8
MMG014	17.5	17.6	8.1	7.8	142.7	137.2
Average ± SD	19.0±1.5	19.2±1.6	8.9±1.2	8.6±1.2	169.1±27.0	164.6±28.1

5.3 TMJ loads (% applied bite force)

For molar biting, the TMJ loads were larger on the contralateral compared to ipsilateral sides in 11 of 12 subjects when the mandible was in retruded position and all subjects when the mandible was protruded to Class I occlusion (Table 4). Overall, the contralateral (left) condyle received significantly higher TMJ loads compared to the ipsilateral (right) condyle during molar biting in the retruded (33.4 ± 4.1 versus 18.6 ± 5.9 % applied BF, respectively; $p<0.0001$), 3 mm protruded (40.0 ± 4.3 versus 12.4 ± 3.9 % applied BF, respectively; $p<0.001$), and 6 mm protruded (36.5 ± 6.2 versus 21.7 ± 5.3 % applied BF, respectively; $p<0.005$) mandibular positions (Figure 7). TMJ loads during molar biting in protruded compared to retruded mandibular positions tended to be smaller on the ipsilateral side (nine of 12 subjects) and larger on the contralateral side (11 of 12 subjects; Table 4). Overall, TMJ loads during molar biting in the 6 mm protruded compared to molar biting in the 3 mm protruded positions were significantly

higher for the ipsilateral condyle (21.7 ± 5.3 versus 12.4 ± 3.9% applied BF, respectively; $p<0.01$) and not significantly different for the contralateral condyle (36.5 ± 6.2 versus 40.0 ± 4.3% applied BF, respectively; $p=0.31$) (Figure 7).

For incisor biting, the TMJ loads were larger on the ipsilateral compared to contralateral sides in all 12 subjects when the mandible was protruded to the Class I occlusion (Table 4). Overall, TMJ loads during incisor biting were not significantly different between ipsilateral and contralateral sides in the 3 mm protruded position (61.4 ± 6.7 versus 53.1 ± 6.1% applied BF, respectively; $p=0.075$) and 6 mm protruded position (65.4 ± 8.7 versus 57.6 ± 8.8% applied BF, respectively; $p=0.12$) (Figure 7). TMJ loads during incisor biting compared to molar biting in the protruded position were larger in all 12 subjects on both ipsilateral and contralateral sides (Table 4). Overall, TMJ loads during incisor biting were significantly higher compared to molar biting in the 3 mm protruded position for the ipsilateral (61.4 ± 6.7 versus 12.4 ± 3.9% applied BF, respectively; $p<0.0001$) and contralateral sides (53.1 ± 6.1 versus 40.0 ± 4.3% applied BF, respectively; $p=0.002$) (Figure 7). TMJ loads during incisor biting were significantly higher compared to molar biting in the 6 mm protruded position as well for the ipsilateral (65.4 ± 8.7 versus 21.7 ± 5.3% applied BF, respectively; $p<0.0001$) and contralateral (57.6 ± 8.8 versus 36.5 ± 6.2% applied BF, respectively; $p<0.0001$) (Figure 7). TMJ loads during incisor biting compared to molar biting in the retruded position were larger in all 12 subjects on both ipsilateral and contralateral sides (Table 4).

Table 4. **Means and standard deviations (SDs) of predicted temporomandibular joint loads (% applied bite force)** for molar biting with mandible retruded and molar and incisor biting with mandible protruded to class I occlusion (3 mm, shown in red font, or 6 mm, shown in blue font, advancement) for subjects before orthodontic treatment.

ID	Temporomandibular Joint Loads (% applied bite force) for					
	Molar Biting in Retruded Position		Protruded to Class I (3 mm or 6 mm)			
			Molar Biting		Incisor Biting	
	Ipsilateral	Contralateral	Ipsilateral	Contralateral	Ipsilateral	Contralateral
MMG001	25.5□8.8	32.5□11.8	25.5□9.3	32.5□13.3	73.5□4.3	49.4□12.4
MMG002	15.4□8.1	37.6□10.1	13.0□6.9	46.8□8.1	67.0□7.3	61.8□7.7
MMG003	24.2□11.2	35.7□13.0	21.2□8.6	42.7□11.6	69.2□9.8	57.9□10.8
MMG004	18.3□10.1	28.3□11.6	17.5□9.3	32.7□13.5	51.6□14.7	47.3□13.8
MMG005	10.0□3.8	34.0□10.5	10.3□3.5	37.0□11.5	59.6□10.6	55.0□12.1
MMG008	19.4□12.2	32.3□10.2	16.8□8.9	38.0□8.7	68.0□5.8	47.3□9.9
MMG009	7.5□5.3	34.0□9.5	7.0□4.6	36.5□10.7	51.3□9.1	47.2□10.3
MMG010	17.7□8.8	29.4□9.6	16.2□8.4	32.9□10.2	55.9□12.8	50.9□12.8
MMG011	27.2□14.1	25.8□11.8	23.5□14.1	32.3□14.3	63.8□17.0	62.7□19.1
MMG012	18.5□6.6	38.4□11.9	19.7□6.0	44.3□13.3	73.5□13.5	71.0□14.1
MMG013	22.5□10.9	33.5□12.3	21.5□9.2	41.7□13.7	70.1□13.7	64.2□15.8
MMG014	16.5□8.9	38.9□8.6	14.9□7.2	41.6□8.3	61.2□7.5	54.2□8.4
Average ± SD	18.6□5.9	33.4□4.1	17.3□5.4	38.3□5.1	63.7□7.8	55.7□7.8

Figure 7. Temporomandibular joint (TMJ) loads (% applied bite-force) during molar and incisor biting with the mandible in the retruded and protruded positions, respectively. Significant differences in TMJ loads illustrated, where significance defined by $p<0.05$.

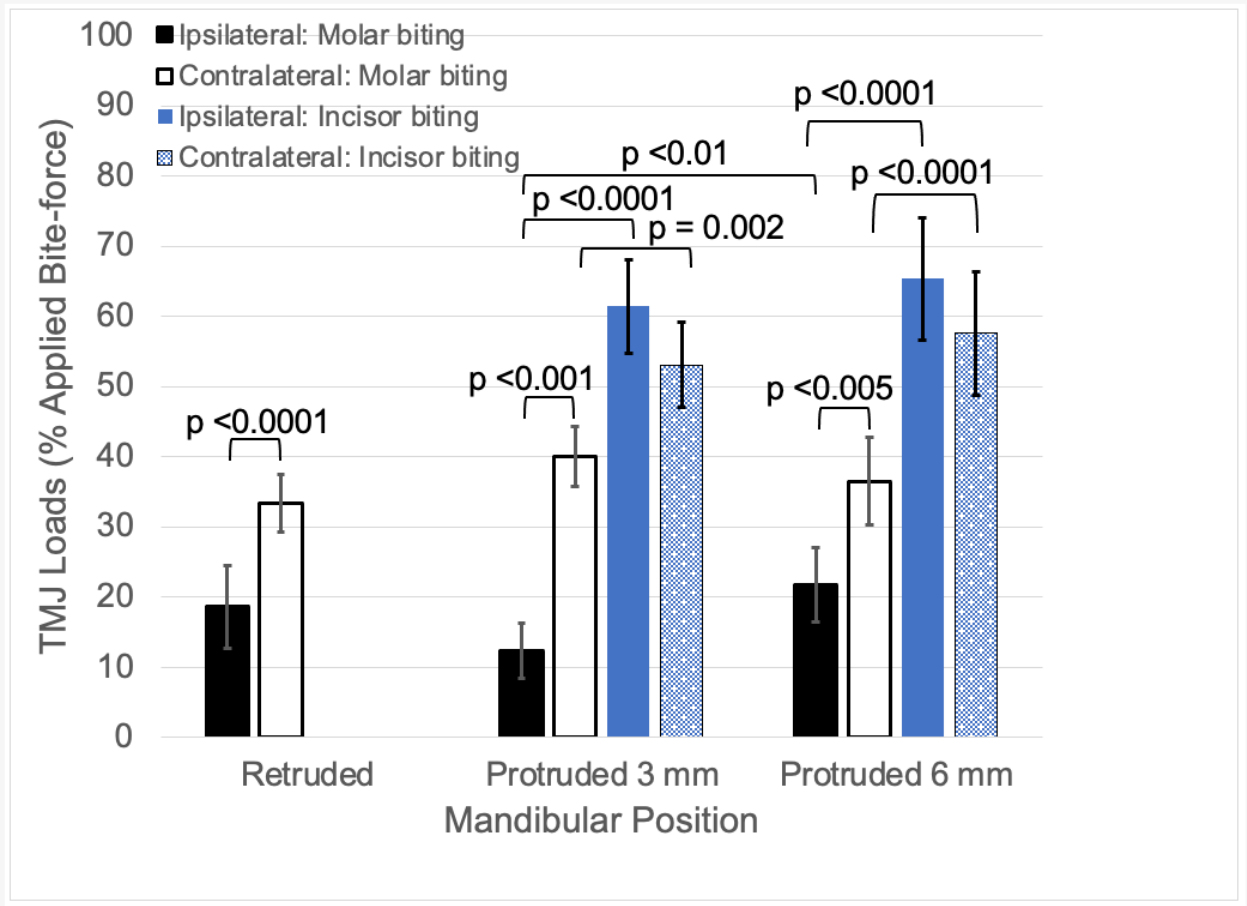

5.4 TMJ compressive stresses (MPa)

For molar biting, the TMJ compressive stresses were also larger on the contralateral compared to ipsilateral sides in 11 of 12 subjects when the mandible was in retruded and in protruded positions (Table 5). Overall, the contralateral condyle received significantly higher TMJ compressive stresses (MPa) compared to the ipsilateral condyle during molar biting in the retruded (0.21 □ 0.06 versus 0.11 □ 0.04 MPa, respectively; $p<0.0001$), 3 mm protruded (0.27 □ 0.06 versus 0.08 □ 0.03 MPa, respectively; $p<0.005$), and 6 mm protruded (0.21 □ 0.04 versus

0.13 □ 0.03 MPa, respectively; p<0.005) mandibular positions (Figure 8). There was no significant difference in TMJ compressive stresses for molar biting between Group A (molar biting in retruded position) and Group B (molar biting in the protruded position (3 mm and 6 mm)) on the ipsilateral (0.11 □ 0.04 versus 0.11 □ 0.04 MPa, respectively; p=0.73) and contralateral (0.21 □ 0.05 versus 0.24 □ 0.05 MPa, respectively; p=0.18) sides (Figure 8).

For incisor biting when the mandible was in a protruded position, the TMJ compressive stresses were larger on the ipsilateral compared to contralateral sides for all 12 subjects (Table 5). However, overall there were no significant differences in TMJ compressive stresses between ipsilateral and contralateral sides for incisor biting (0.37 □ 0.13 versus 0.34 □ 0.07 MPa, respectively; p=0.54). Incisor biting yielded significantly higher compressive stresses compared to molar biting in the protruded mandibular position (3 mm and 6 mm) for both ipsilateral (0.37 □ 0.13 versus 0.11 □ 0.04 MPa, respectively; p<0.0001) and contralateral condyles (0.34 □ 0.07 versus 0.24 □ 0.05 MPa, respectively; p<0.001) (Figure 8).

Table 5. Means and standard deviations (SDs) of predicted temporomandibular joint compressive stresses (MPa) for molar biting with mandible retruded and molar and incisor biting with mandible protruded to class I occlusion (3 mm, shown in red font, or 6 mm, shown in blue font, advancement) for subjects before orthodontic treatment.

ID	Temporomandibular Joint Compressive Stresses (MPa) for					
	Molar Biting in Retruded Position		Protruded to Class I (3 mm or 6 mm)			
			Molar Biting		Incisor Biting	
	Ipsilateral	Contralateral	Ipsilateral	Contralateral	Ipsilateral	Contralateral
MMG001	0.14□0.05	0.18□0.07	0.18□0.05	0.16□0.08	0.40□0.02	0.27□0.07
MMG002	0.11□0.06	0.28□0.07	0.10□0.05	0.34□0.06	0.49□0.05	0.46□0.06
MMG003	0.12□0.06	0.18□0.07	0.11□0.04	0.22□0.06	0.35□0.05	0.30□0.06
MMG004	0.09□0.05	0.14□0.06	0.09□0.05	0.17□0.07	0.26□0.07	0.24□0.07
MMG005	0.07□0.02	0.24□0.08	0.07□0.02	0.26□0.09	0.42□0.07	0.39□0.09
MMG008	0.11□0.06	0.18□0.06	0.09□0.05	0.21□0.05	0.38□0.03	0.26□0.06
MMG009	0.04□0.03	0.17□0.05	0.04□0.03	0.19□0.05	0.27□0.05	0.25□0.05
MMG010	0.14□0.07	0.24□0.08	0.13□0.07	0.27□0.08	0.45□0.10	0.41□0.11
MMG011	0.18□0.09	0.17□0.08	0.15□0.09	0.21□0.09	0.42□0.11	0.41□0.12
MMG012	0.10□0.04	0.20□0.06	0.10□0.03	0.24□0.07	0.39□0.07	0.38□0.07
MMG013	0.13□0.07	0.19□0.07	0.12□0.06	0.24□0.08	0.41□0.08	0.37□0.09
MMG014	0.12□0.06	0.28□0.06	0.11□0.06	0.30□0.06	0.44□0.05	0.39□0.06
Average □ SD	0.11□0.04	0.20□0.05	0.11□0.04	0.23□0.05	0.39□0.07	0.34□0.08

Figure 8. Temporomandibular joint (TMJ) compressive stresses (MPa) during molar and incisor biting with the mandible in the retruded and protruded positions, respectively. Significant differences in TMJ compressive stresses illustrated, where significance defined by $p<0.05$.

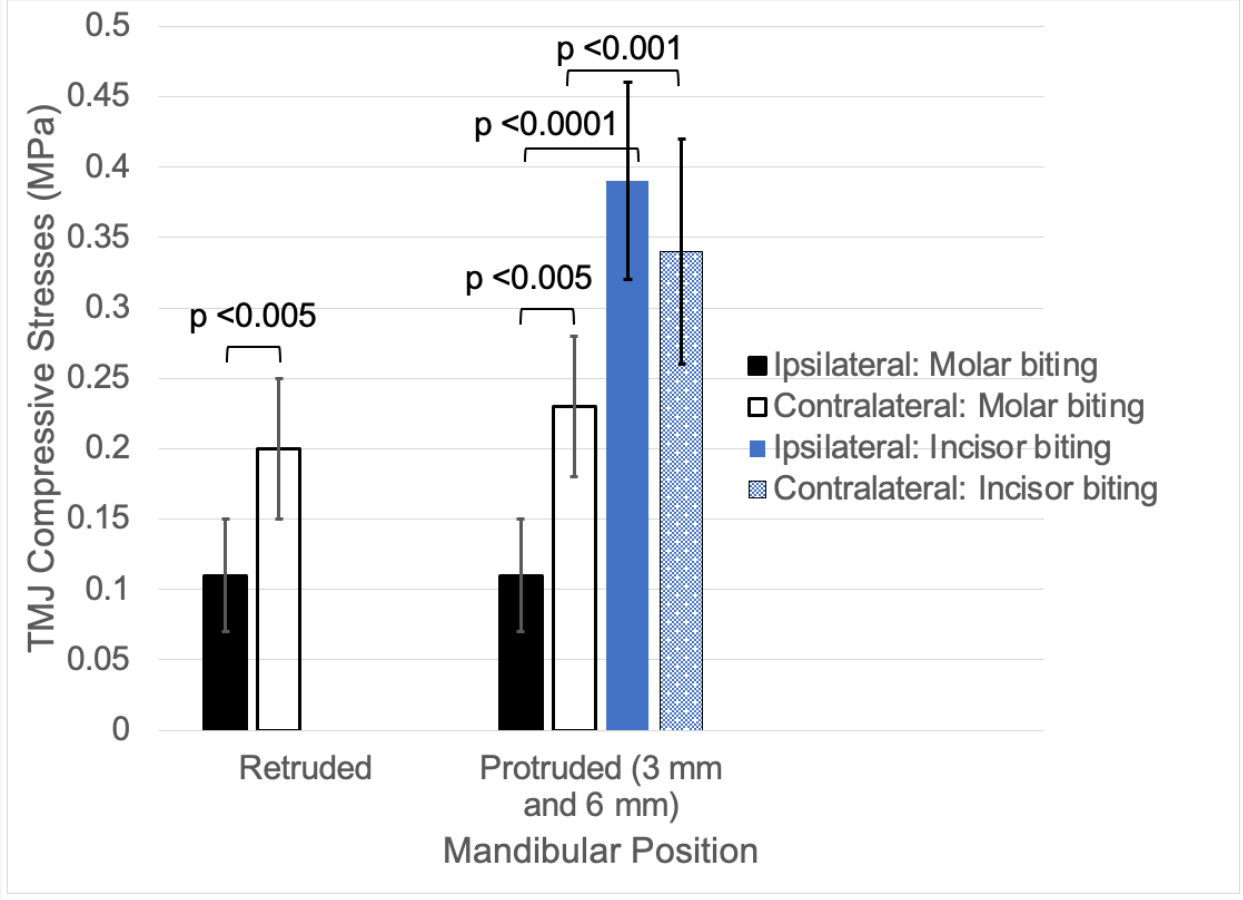

5.5 Association with sample variables

There were no significant differences in compressive stresses for ipsilateral or contralateral condyles during incisor or molar biting between males and females (all $p>0.05$).

Regression analyses of TMJ load (%) for molar biting versus mandible length (mm), and Co-Go length (mm) on the same side showed positive correlations for both ipsilateral ($R^2 = 0.69$; Figure 7) and contralateral TMJs ($R^2 = 0.46$; Figure 8). That is, higher ipsilateral joint loads were

correlated with increased mandibular length and decreased Co-Go length on the right; whereas, higher contralateral joint loads were correlated with decreased mandibular length and increased Co-Go length on the left. Regression analyses of TMJ load (%) for incisor biting versus mandible length (mm), and Co-Go length (mm) on the same side showed positive correlations for both ipsilateral ($R^2 = 0.24$, Figure 9) and contralateral TMJs ($R^2 = 0.30$, Figure 10) and followed similar trends – higher ipsilateral joint loads were correlated with increased mandibular length and decreased Co-Go length on the right, and higher contralateral joint loads were correlated with decreased mandibular length and increased Co-Go length on the left.

Regression analysis of the independent variables of age (years) and ipsilateral condyle stress (MPa) for molar biting in the retruded position, and the dependent variable mandible length (mm) showed a positive correlation ($R^2 = 0.52$; Figure 11). That is, longer mandibular lengths were found in older subjects with lower ipsilateral condyle stresses during biting, where specifically for the group, those with the longest mandibular lengths tended to be at least 14 years old and have ipsilateral condyle stresses of < 0.12 MPa.

Figure 9. 3D regression analysis of ipsilateral TMJ load (% applied bite force) during molar biting in retruded mandibular position, versus mandibular length (mm), and ramal length (Co-Go length, mm).

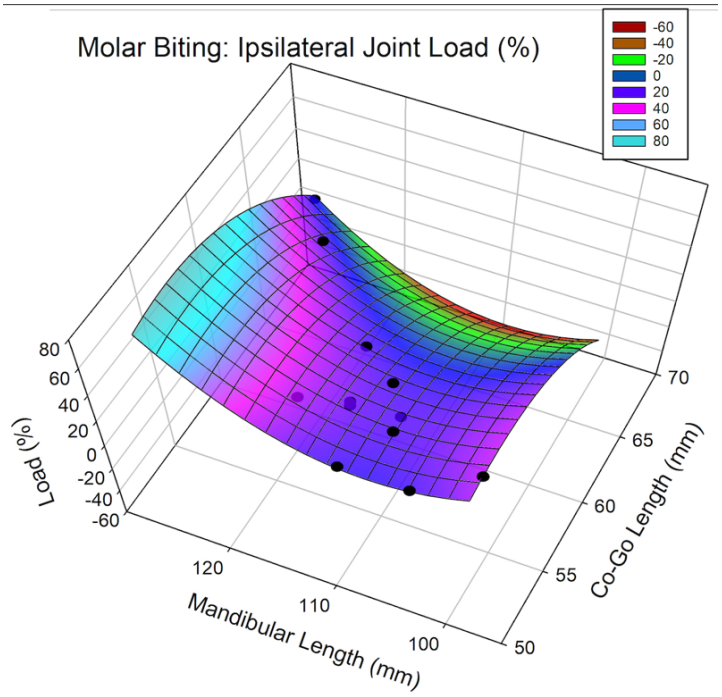

Figure 10. 3D regression analysis of contralateral TMJ load (% applied bite force) during molar biting in retruded mandibular position, versus mandibular length (mm), and ramal length (Co-Go length, mm).

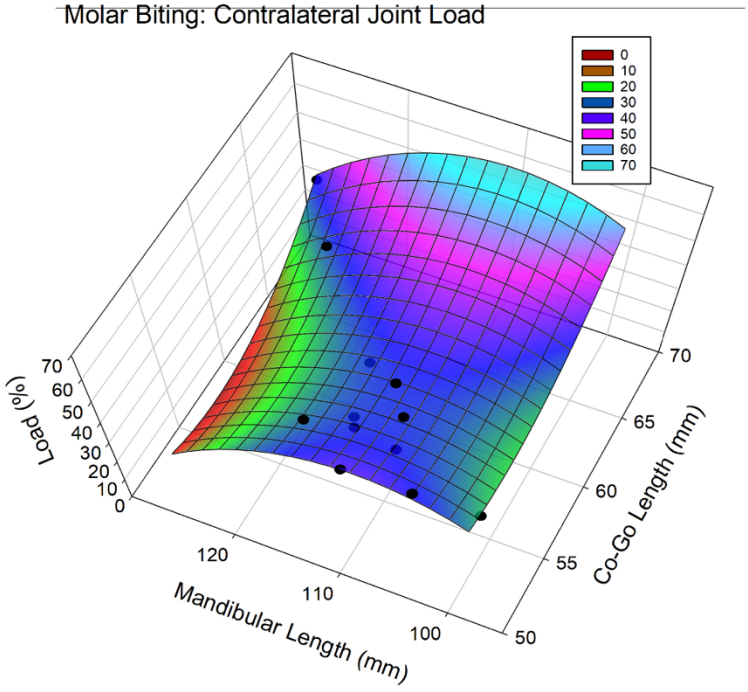

Figure 11. 3D regression analysis of ipsilateral TMJ load (% applied bite force) during incisor biting in protruded mandibular position, versus mandibular length (mm), and ramal length (Co-Go length, mm).

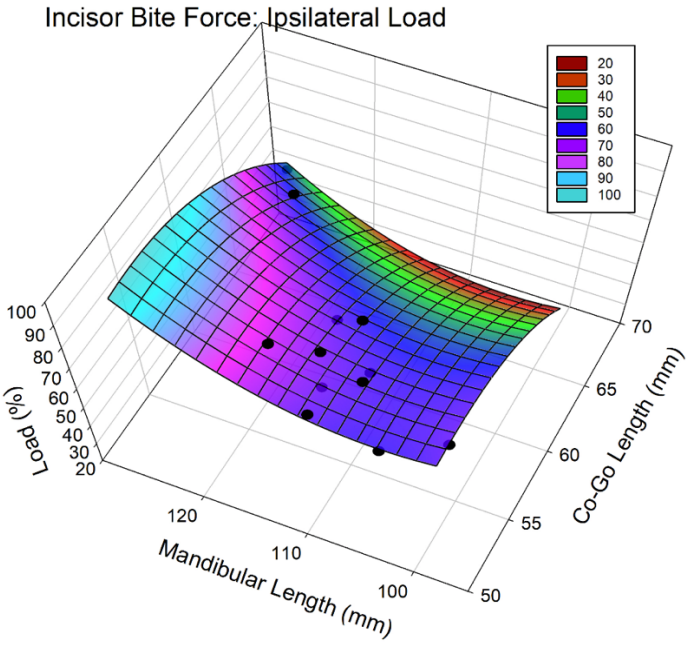

Figure 12. 3D regression analysis of contralateral TMJ load (% applied bite force) during incisor biting in protruded mandibular position, versus mandibular length (mm) and ramal length (Co-Go length, mm).

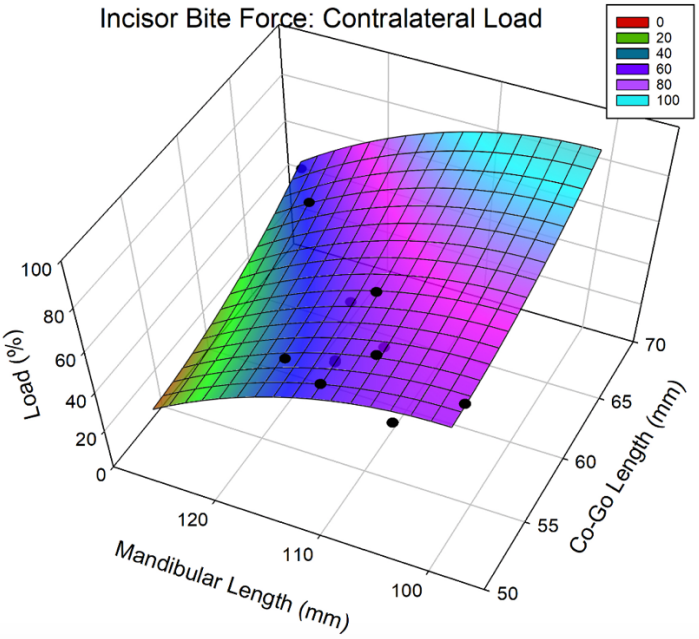

Figure 13. 3D regression analysis of mandible length (mm) versus age (years) and ipsilateral condyle stress (MPa) for molar biting in retruded mandibular position.

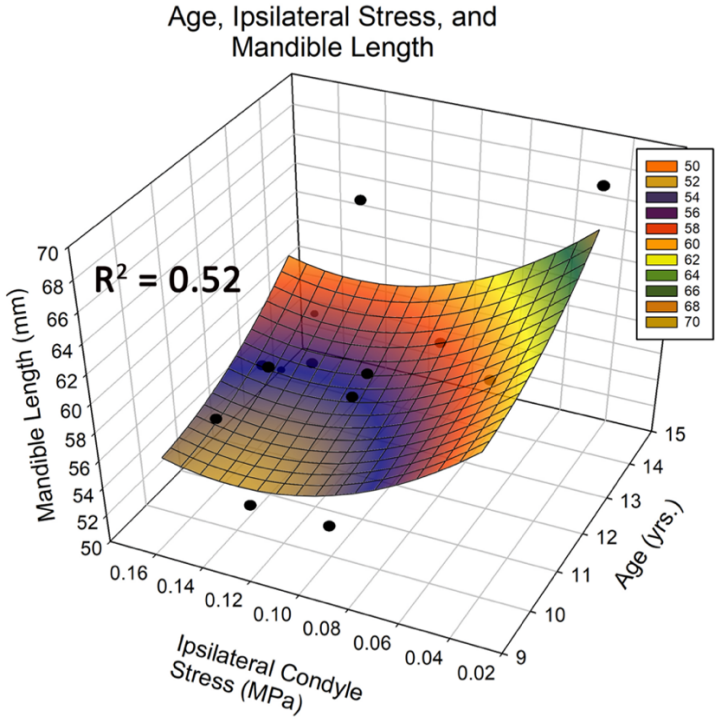

6) Discussion

This study further demonstrates the associations between joint loads and mandibular lengths in a pediatric population. Regression analysis showed a positive correlation with ipsilateral condyle (compressive) stress, age, and mandible length. That is, relatively longer mandibular lengths were associated with relatively increased age and lower ipsilateral condylar stress, specifically in this sample <0.12 MPa. These findings were consistent with data from a retrospective longitudinal study[24] which showed that predicted TMJ compressive stresses during incisor biting increased with age between 6 – 18 years and were non-linearly related to ramal lengths, suggesting a theoretical threshold of stress (0.05 – 0.10 MPa) above which was associated with possible inhibition of condylar cartilage growth. This is in agreement with data from condyle

explant studies[15] where increased static compressive stresses resulted in decreased metabolism of secondary cartilage and cessation of mandibular cartilage growth.

Contralateral TMJ loads and stresses were significantly greater than ipsilateral TMJ loads and stresses in both males and females during unilateral molar biting at all mandibular positions tested (retruded and protruded to Class I occlusion). This asymmetric loading could be due to the unilateral bite task of biting on the right mandibular first molar, requiring translation of the contralateral condyle and resultant greater TMJ load compared to simple rotational movement of the ipsilateral condyle. When the bite task was more centered and symmetric, as in incisor biting in the protruded mandibular position, there were no significant differences between contralateral and ipsilateral TMJ loads in the 3 mm ($p=0.075$) and 6 mm ($p=0.12$) protruded positions and compressive stresses ($p=0.54$).

The trends from regression analyses regarding joint loads and mandibular lengths were unexpected. Notably, for both unilateral molar and incisor biting, the lowest ipsilateral TMJ loads in the group were associated with the longest ramal lengths (Co-Go; Figures 7 and 9), while the lowest contralateral TMJ loads were associated with the longest mandibular lengths (Figures 8 and 10). This suggests that the geometrical anatomy of the mandible and vectors of masticatory muscle force may affect the condyles differently with respect to TMJ loading during jaw functions, and ultimately could affect ramal and mandibular lengths. This emphasizes the complexity of the masticatory system – different effects may be felt on each condyle during the same biting task.

The finding that TMJ loads were not very different during molar biting with the mandible in retruded compared to protruded positions of either 3 mm or 6 mm (average changes for ipsilateral and contralateral TMJ loads were -1.3 and +4.9 MPa, respectively; Table 4) suggested that for these subjects, unilateral molar biting in Class II versus Class I position did not markedly change the predicted TMJ loads on either side. Because, for a given subject and TMJ, the same estimated condylar area was used for both retruded and protruded positions, not surprisingly, estimated TMJ compressive stresses during unilateral molar biting with the mandible in the retruded compared to protruded positions showed similar trends. This is different than expected in vivo and an explanation for this is likely due to a limitation in the calculation of compressive stresses. A constant estimated subject-specific maximum condylar loading area was used in the calculation of compressive stresses in both retruded and protruded mandibular positions, that was a "best-case" scenario for stress distribution. However, this failed to account for the degree of matching, also known as congruence, between the articular surfaces of fossa and condyle, which affects the area over which the compressive stress is applied during biting. This congruence is the result of an individual's specific anatomy and relative positions of the condyle, which can rotate and translate during normal jaw functions. In general, the main condylar axis in humans is not perpendicular to the sagittal plane; therefore, for symmetrical movements, this axis is not perpendicular to the main direction of condylar movement and tends to enhance the surface-mismatching or incongruency during these movements. It has been shown in a study using three-dimensional reconstructions of TMJs with magnetic resonance imaging (MRIs) and jaw tracking data that the higher concentration of work done (energy density) to the TMJ disc during asymmetric compared to symmetric mandibular movements, such as lateral excursions of the mandible compared to symmetric jaw-opening and jaw-closing, is likely due to this

incongruence.[25] A more specific measure of the size of the stress-field of the TMJ loaded contact sites for each TMJ in each subject in the retruded and protruded mandibular positions as described in a previous study[17] would have improved the accuracy of the predicted compressive stresses. It is postulated that the measured stress-field area would have been smaller in the protruded versus retruded mandibular positions due to the expected greater incongruency between the surfaces of the condylar head with the temporal fossa versus with the eminence. Thus, although the current study showed that TMJ loads were not significantly different during unilateral molar biting with the mandible in retruded compared to protruded positions, if the stress field was relatively smaller in protruded position, the compressive stresses would have been larger in the protruded compared to retruded mandibular positions.

Although protrusion of the mandible 3 – 6 mm during unilateral molar biting did not significantly affect the TMJ loads on either side, incisor biting in the protruded mandibular position yielded significantly higher TMJ loads and stresses compared to molar biting in the protruded mandibular position (all $p \leq 0.002$ and $p < 0.001$, respectively). This can be explained by the anatomic geometry of the mandible – incisor biting occurs at a longer distance from the TMJ contact sites compared to molar biting, thereby creating a greater moment and higher loads at the TMJ contact sites than would molar biting given the same biting task. If the aim is to increase TMJ loading for the same applied bite-force, this suggests it would be more effective to bite on the incisors than the molars in the protruded position.

The molecular biological perspective of TMJ loading should be considered in regards to compressive stresses. Mechanical loads, in a dose-dependent manner with respect to magnitude

and frequency, inhibit or promote molecular events responsible for cartilage health or destruction, involving the synthesis of inflammatory mediators.[6,26-28] Excessive loading and subsequent inflammatory mediators are associated with increased Wnt signaling in the superficial zone of the TMJ fibrocartilage and loss of fibrocartilage stem cells in this zone.[29] Given these findings, the modulation of compressive stresses through mandibular protrusion may play a role in the modulation of growth at the condyle.

The current study compared TMJ compressive stresses during unilateral molar biting in the retruded and protruded mandibular positions and incisor biting in the protruded mandibular positions, where the amount of protrusion simulated what would be expected during Herbst appliance therapy. TMJ compressive stresses relate to the magnitude of jaw loading behaviors. However, it is known that the mechanosensitivity of the growing condyle is vulnerable both to the magnitude and frequency of jaw loading behaviors. For a more accurate analysis of the frequency of jaw loading behaviors, durations of jaw muscle activities could be measured as well using ambulatory electromyography (EMG). A more comprehensive representation of jaw loading behaviors could include a calculation of energy densities (measure of the mechanical work input per volume between the condyle and temporal eminence loading areas, mJ/mm^3) and jaw muscle duty factors (muscle activity duration/total recording time, %) as described by a previous study.[16] A mechanobehavior score (MBS) can then be calculated as a product of the magnitude and frequency of jaw loading behaviors ($MBS=ED^2xDF$, $(\frac{mJ}{mm^3})^2\%$) to more accurately represent what would be expected during Herbst appliance therapy.

This study had limitations because the accuracy of model-predicted TMJ loads and compressive stresses could not be validated. A small sample size of subjects made comparisons between sexes difficult and FHMPA distinguishing brachyfacial, dolichofacial, and mesofacial phenotypes impossible. A limited number of subjects completed their Herbst treatment prior to the completion of this thesis; therefore, a comparison of measurements at different timepoints pre- and post-treatment could not be made. These shortcomings could be addressed through a continuation of this prospective longitudinal study with the recruitment of more subjects with more timepoints post-treatment to assess correlations in condylar loading and changes in mandibular and ramal lengths. Mechanobehavior scores (MBS) can be calculated to encompass both the magnitude and frequency of jaw loading behaviors as described in previous literature.[16,17] More ideally, an identical twin study could compare clinical outcomes of functional appliances with unaltered growth if the twins could be assigned to different groups who received and did not receive jaw orthopedic treatment. Although ideal, it would be challenging to find sets of identical twin subjects with similar malocclusions, environments, and jaw loading behaviors, who would also agree to be treated differently.

In a hypothetical model, if the components of jaw loading control the amount of growth of the condyles in children, modulation of jaw loading behaviors could be prescribed by orthodontists to facilitate condylar growth for ideal jaw relations. A theoretical mechanical threshold of compressive stress of around 0.05 – 0.10 MPa has been suggested[6,24] (Figure 4), below which chondrogenesis is promoted and above which chondrogenesis is inhibited. A similar threshold magnitude was found to be related to mandibular length in the current study. Magnitude of jaw loading could be modulated towards this threshold with mandibular repositioning, for example

with orthodontic functional appliances or reduced biting on incisors. Frequency of jaw loading could be modulated with changes in jaw loading behavior, for example the frequency of chewing gum. Ultimately, further evidence is needed to elucidate the associations between these jaw loading components and condylar growth.

7) Conclusions

In a pediatric population before orthodontic treatment: 1A. Predicted TMJ loads (% applied bite force) and 1B. TMJ compressive stresses (MPa) were significantly greater during unilateral incisor biting with the mandible protruded to class I occlusion compared to unilateral molar biting with the mandible in the retruded and protruded positions, but not different during unilateral molar biting with the mandible in protruded compared to retruded position; 2A. Both ipsilateral and contralateral TMJ loads for unilateral biting on molars with the mandible in retruded position and incisors with the mandible in protruded position were positively correlated with mandibular and ramal lengths; and 2B. increased age and decreased ipsilateral TMJ compressive stress were non-linearly correlated with increased mandibular length. Thus, increased age in the range between 10-14 years and relatively lower ipsilateral TMJ compressive stresses may be possible pre-treatment clinical indicators of predicting success with mandibular orthopedic appliances.

References

1. Ricketts RM. A foundation for cephalometric communication. *American Journal of Orthodontics.* 1960/05/01/ 1960;46(5):330-357.
2. Karlsen AT. Association between facial height development and mandibular growth rotation in low and high MP-SN angle faces: a longitudinal study. *Angle Orthod.* 1997;67(2):103-110.
3. Iwasaki LR, Liu Y, Liu H, Nickel JC. Jaw mechanics in dolichofacial and brachyfacial phenotypes: A longitudinal cephalometric-based study. *Orthodontics & Craniofacial Research.* 2017;20(S1):145-150.
4. Gallo LM, Iwasaki LR, Gonzalez YM, Liu H, Marx DB, Nickel JC. Diagnostic group differences in temporomandibular joint energy densities. *Orthod Craniofac Res.* Apr 2015;18 Suppl 1(0 1):164-169.
5. Kuo J, Shi C, Cisewski S, Zhang L, Kern MJ, Yao H. Regional cell density distribution and oxygen consumption rates in porcine TMJ discs: an explant study. *Osteoarthritis and Cartilage.* 2011-07-01 2011;19(7):911-918.
6. Nickel JC, Iwasaki LR, Gonzalez YM, Gallo LM, Yao H. Mechanobehavior and Ontogenesis of the Temporomandibular Joint. *Journal of Dental Research.* 2018-10-01 2018;97(11):1185-1192.
7. Nickel JC, McLachlan KR. An analysis of surface congruity in the growing human temporomandibular joint. *Archives of Oral Biology.* 1994;39(4):315-321.
8. DeVincenzo JP. Changes in mandibular length before, during, and after successful orthopedic correction of Class II malocclusions, using a functional appliance. *American Journal of Orthodontics and Dentofacial Orthopedics.* 1991/03/01/ 1991;99(3):241-257.
9. Deen E, Woods MG. Effects of the Herbst appliance in growing orthodontic patients with different underlying vertical patterns. *Australasian Orthodontic Journal.* 2015-01-01 2015;31(1):59-68.
10. Hedlund C, Feldmann I. Success rate, costs and long-term stability of treatment with activator/headgear combinations. *Swed Dent J.* 2016;40(1):67-77.
11. King GJ, McGorray SP, Wheeler TT, Dolce C, Taylor M. Comparison of peer assessment ratings (PAR) from 1-phase and 2-phase treatment protocols for class II malocclusions. *American Journal of Orthodontics and Dentofacial Orthopedics.* 2003/05/01/ 2003;123(5):489-496.
12. O'Brien K, Wright J, Conboy F, et al. Effectiveness of treatment for Class II malocclusion with the Herbst or twin-block appliances: a randomized, controlled trial. *Am J Orthod Dentofacial Orthop.* Aug 2003;124(2):128-137.
13. Tulloch JF, Proffit WR, Phillips C. Outcomes in a 2-phase randomized clinical trial of early Class II treatment. *Am J Orthod Dentofacial Orthop.* Jun 2004;125(6):657-667.
14. Karlo CA, Stolzmann P, Habernig S, Müller L, Saurenmann T, Kellenberger CJ. Size, shape and age-related changes of the mandibular condyle during childhood. *Eur Radiol.* Oct 2010;20(10):2512-2517.
15. Copray JC, Jansen HW, Duterloo HS. Growth and growth pressure of mandibular condylar and some primary cartilages of the rat in vitro. *Am J Orthod Dentofacial Orthop.* Jul 1986;90(1):19-28.

16. Riddle PC, Nickel JC, Liu Y, et al. Mechanobehavior and mandibular ramus length in different facial phenotypes. *Angle Orthod.* Nov 1 2020;90(6):866-872.
17. Gallo LM, Fankhauser N, Gonzalez YM, et al. Jaw closing movement and sex differences in temporomandibular joint energy densities. *J Oral Rehabil.* Feb 2018;45(2):97-103.
18. Wong RW, Alkhal HA, Rabie AB. Use of cervical vertebral maturation to determine skeletal age. *Am J Orthod Dentofacial Orthop.* Oct 2009;136(4):484.e481-486; discussion 484-485.
19. Fudalej P, Bollen AM. Effectiveness of the cervical vertebral maturation method to predict postpeak circumpubertal growth of craniofacial structures. *Am J Orthod Dentofacial Orthop.* Jan 2010;137(1):59-65.
20. Iwasaki LR, Crosby MJ, Marx DB, et al. Human temporomandibular joint eminence shape and load minimization. *J Dent Res.* Jul 2010;89(7):722-727.
21. Nickel JC, Weber AL, Covington Riddle P, Liu Y, Liu H, Iwasaki LR. Mechanobehaviour in dolichofacial and brachyfacial adolescents. *Orthod Craniofac Res.* Jun 2017;20 Suppl 1:139-144.
22. Nickel JC, Gonzalez YM, McCall WD, et al. Muscle organization in individuals with and without pain and joint dysfunction. *J Dent Res.* Jun 2012;91(6):568-573.
23. Nickel JC, Iwasaki LR, Walker RD, McLachlan KR, McCall WD. Human Masticatory Muscle Forces during Static Biting. *Journal of Dental Research.* 2003;82(3):212-217.
24. Desai RJ, Iwasaki LR, Kim SM, Liu H, Liu Y, Nickel JC. A theoretical analysis of longitudinal temporomandibular joint compressive stresses and mandibular growth. *Angle Orthod.* Jan 1 2022;92(1):11-17.
25. Gallo LM, Chiaravalloti G, Iwasaki LR, Nickel JC, Palla S. Mechanical Work during Stress-field Translation in the Human TMJ. *Journal of Dental Research.* 2006;85(11):1006-1010.
26. Correro-Shahgaldian MR, Ghayor C, Spencer ND, Weber FE, Gallo LM. A Model System of the Dynamic Loading Occurring in Synovial Joints: The Biological Effect of Plowing on Pristine Cartilage. *Cells Tissues Organs.* 2014;199(5-6):364-372.
27. Knobloch TJ, Madhavan S, Nam J, Agarwal J, Suresh, Agarwal S. Regulation of Chondrocytic Gene Expression by Biomechanical Signals. 2008-02-27 2008;18(2):139-150.
28. Schätti OR, Marková M, Torzilli PA, Gallo LM. Mechanical Loading of Cartilage Explants with Compression and Sliding Motion Modulates Gene Expression of Lubricin and Catabolic Enzymes. *CARTILAGE.* 2015;6(3):185-193.
29. Embree MC, Iwaoka GM, Kong D, et al. Soft tissue ossification and condylar cartilage degeneration following TMJ disc perforation in a rabbit pilot study. *Osteoarthritis Cartilage.* Apr 2015;23(4):629-639.

Appendices

Appendix A: Institutional Review Board Approval

APPROVAL OF SUBMISSION

June 3, 2019

Dear Investigator:

On 6-3-2019, the IRB reviewed the following submission:

IRB ID:	STUDY00019761
Type of Review:	Initial Study
Title of Study:	Mechanobehavior distinguishes mandibular growth difference in two facial types
Principal Investigator:	Laura Iwasaki
Funding:	Name: DHHS NIH Natl Inst of Dental & Craniofacial Rsch, PPQ #: 1015455
IND, IDE, or HDE:	None
Documents Reviewed:	• Recording Log • Consent and Authorization Form • HIPAA- Prep to Research Form_MBS & jaw growth.docx • e-appl_R01resub_LI.pdf • Assent Form • Biorecorder Diary • Biorecorder Manual • Subject Calibration Log • Protocol

The IRB granted final approval on 6/3/2019. The study requires you to submit a check-in before 6/2/2020.

Review Category: Expedited Category # 1b, 4, 5, and 6

Copies of all approved documents are available in the study's **Final** Documents (far right column under the documents tab) list in the eIRB. Any additional documents that require an IRB signature (e.g. IIAs and IAAs) will be posted when signed. If this applies to your study, you will receive a notification when these additional signed documents are available.

Appendix B: Custom Cephalometric Analysis

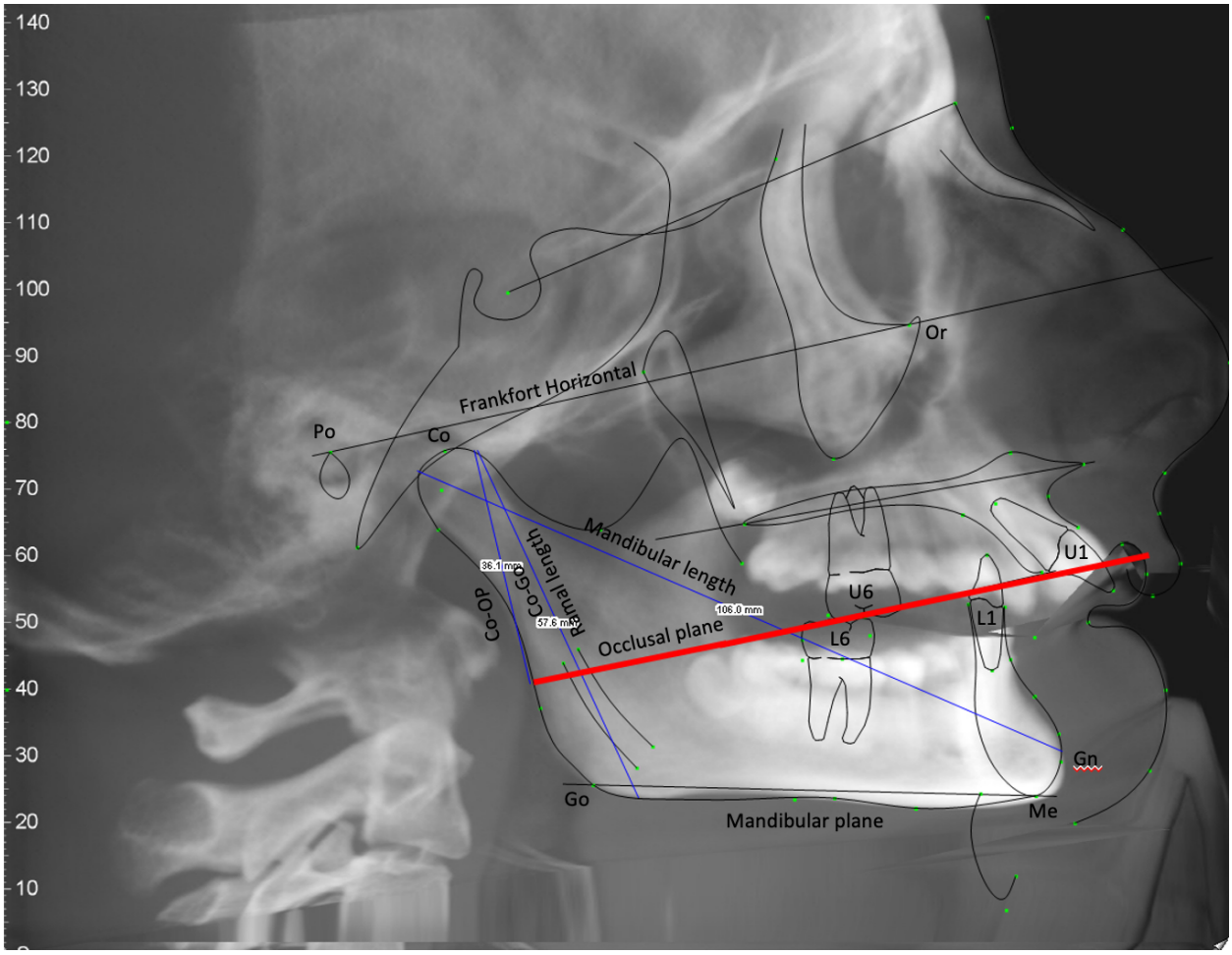

Traced Lateral Cepahlogram Example – showing landmarks as listed below.

From the CBCT-derived lateral cephalogram, the following cephalometric landmarks were used:

- Porion (Po)
- Orbitale (Or)
- Condylion (Co)
- Gonion (Go)
- Menton (Me)
- Gnathion (Gn)
- Maxillary first molar (U6)
- Maxillary central incisor (U1)
- Mandibular first molar (L6)
- Mandibular central incisor (L1)

Using the listed landmarks, the following measurements, reference lines, angles were used:

- Frankfort Horizontal (FH): Porion to Orbitale
- Mandibular plane (MP): Gonion to Menton

- FHMPA (□): Angle between FH and MP
- Occlusal plane: Line bisecting molars (U6/L6) and incisors (U1/L1)
- Ramal length (mm): Condylion to Gonion
- Mandibular length (mm): Maximum length of condyle to chin

Appendix C: Geometry File Landmarks

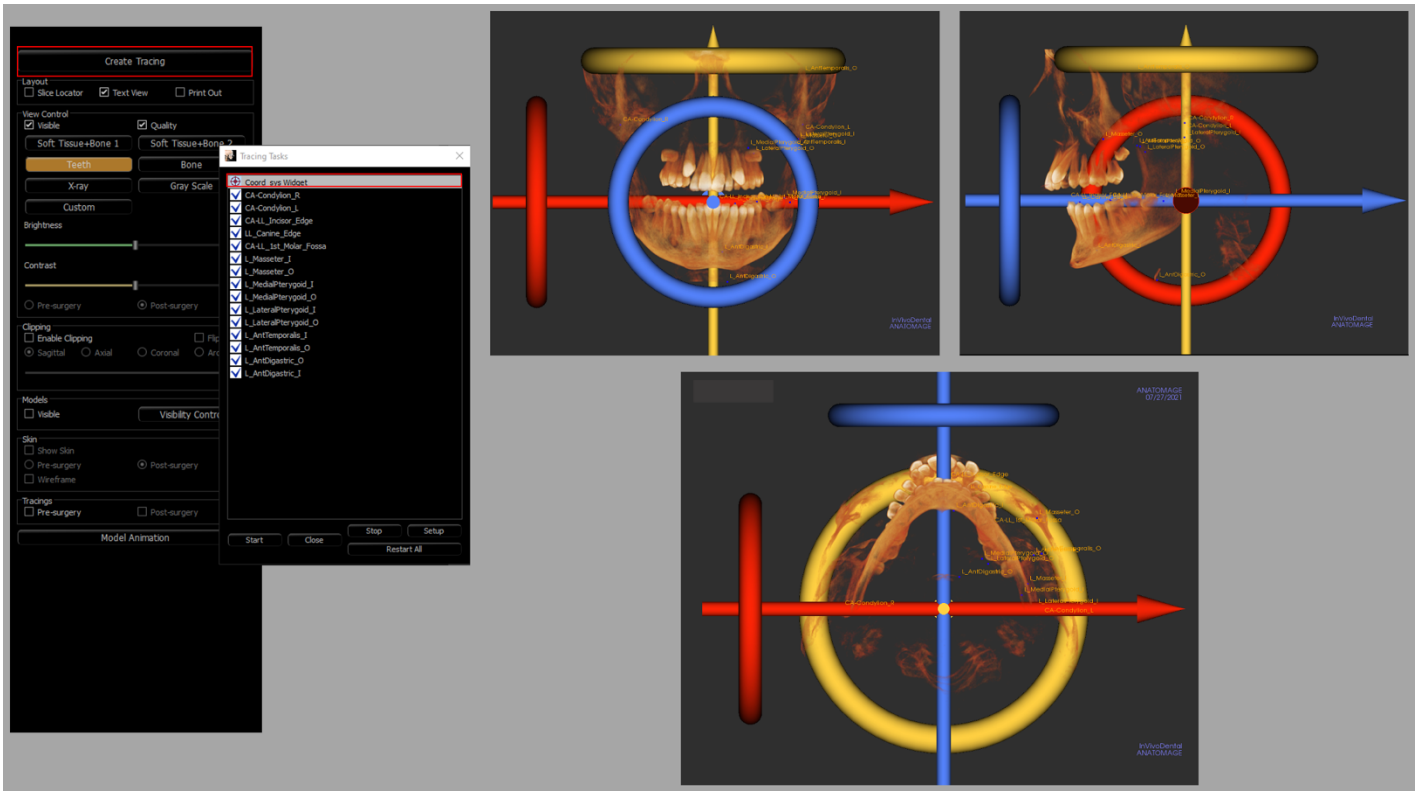

Figure 1: Coordinate planes established using coordinate system widget (Coord_sys_Widget) on InVivo Anatomage. Using the 3DAnalysis feature, cone beam computed tomography (CBCT) calibrated such that the following coordinate planes established: axial (x-z) plane along best fit of mandibular occlusal plane (blue line), coronal (y-z) plane intersecting right and left condylions and perpendicular to occlusal plane (red line), and midsagittal (x-y) plane bisecting inter-condylion distance and perpendicular to axial and coronal planes.

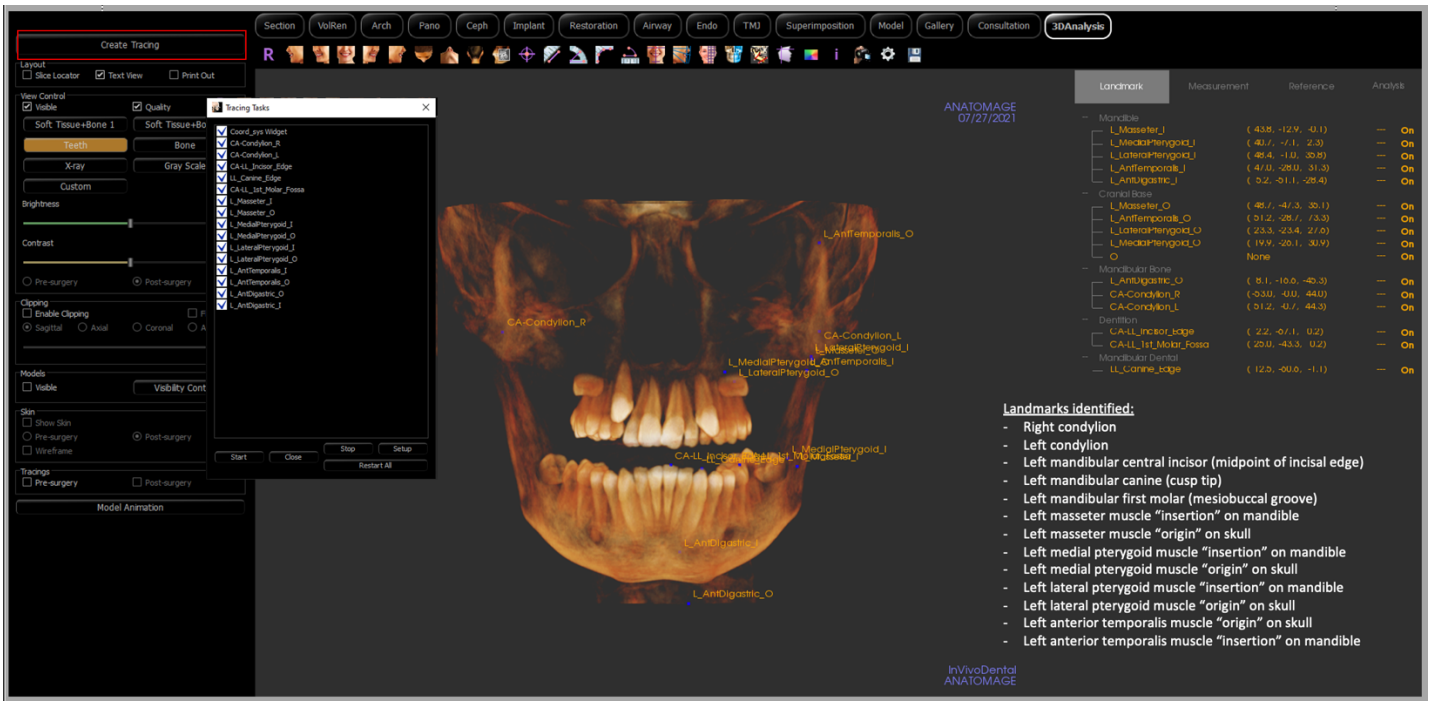

Figure 2: 3D landmarks (blue points) identified on CBCT with InVivo Anatomage. Using 3DAnalysis feature, condyles, teeth, and insertions of muscles of mastication identified.

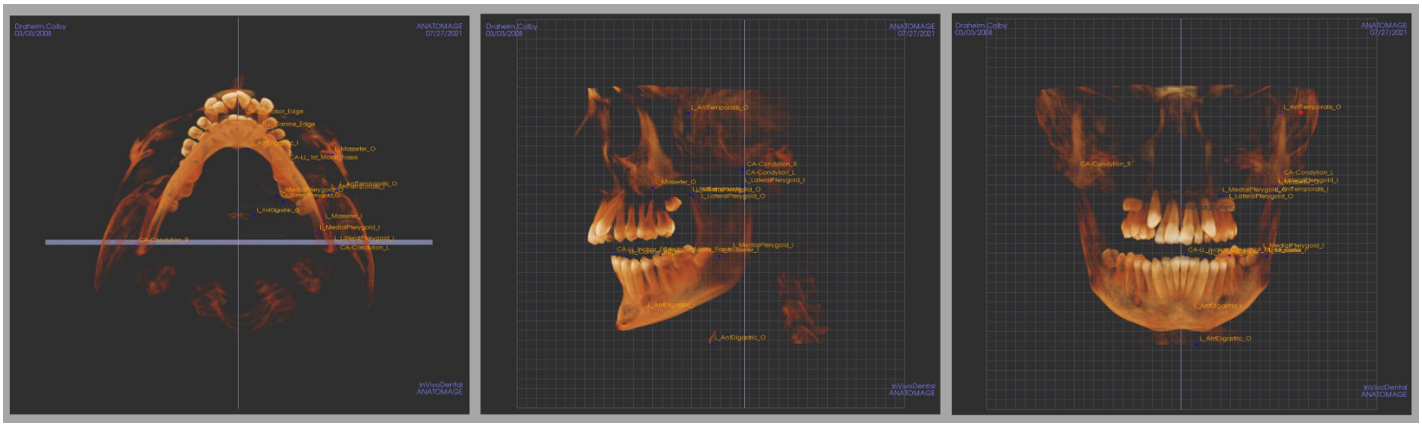

Figure 3: Resultant screenshots of the traced CBCT in the axial, lateral, and posteroanterior, respectively, views to be used in the creation of anatomical geometry files. Grid planes visualized.

Appendix D: Estimated Condylar Loading Area

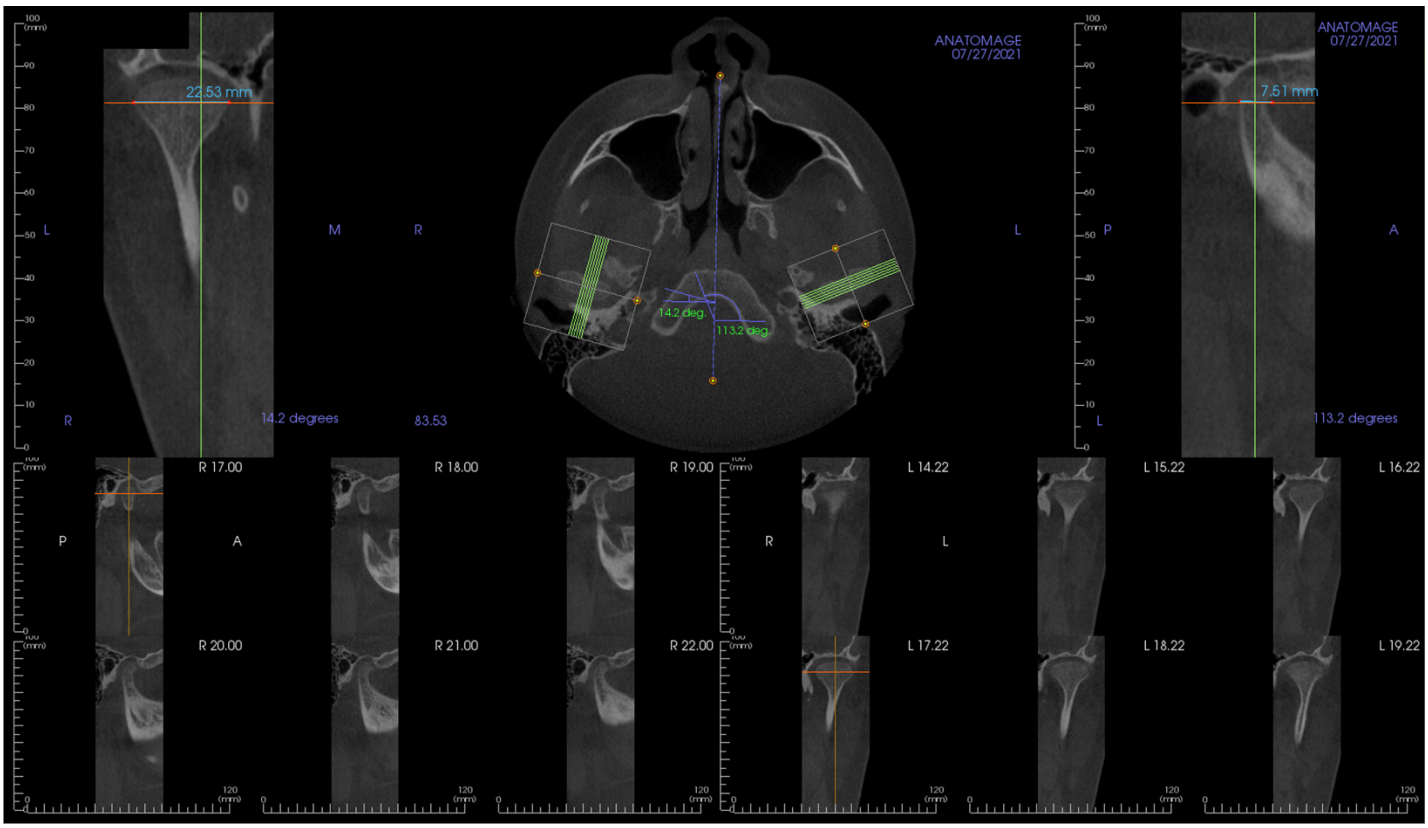

Selected slices of the temporomandibular joint and axial slice of the head (top middle) visualizing the superior aspect of the condyles from cone beam computed tomographic image of the head of one subject. Bottom row of images visualize perpendicular cross-sectional slices of the condyle (shown in green). Major condylar axis was measured as the longest medial-lateral pole distance in a plane parallel to the occlusal plane in the frontal view of the condyle (top left image). Minor condylar axis was measured as the shortest distance perpendicular to the major condylar axis in the same plane (top right image). Each condyle was measured separately – measurements of both condyles in the same plane as seen in the axial slice of the head (top middle) were made only for visualization of both major and minor condylar axes.